UiT
NORGES
ARKTISKE
UNIVERSITET

Department of Engineering and Safety

Finite element analysis of materials for aquaculture net cages

FEA of materials for aquaculture net cages using ANSYS Workbench®

—

Odd Einar Lockertsen Myrli

Master in Technology and Safety in the High North, June 2017

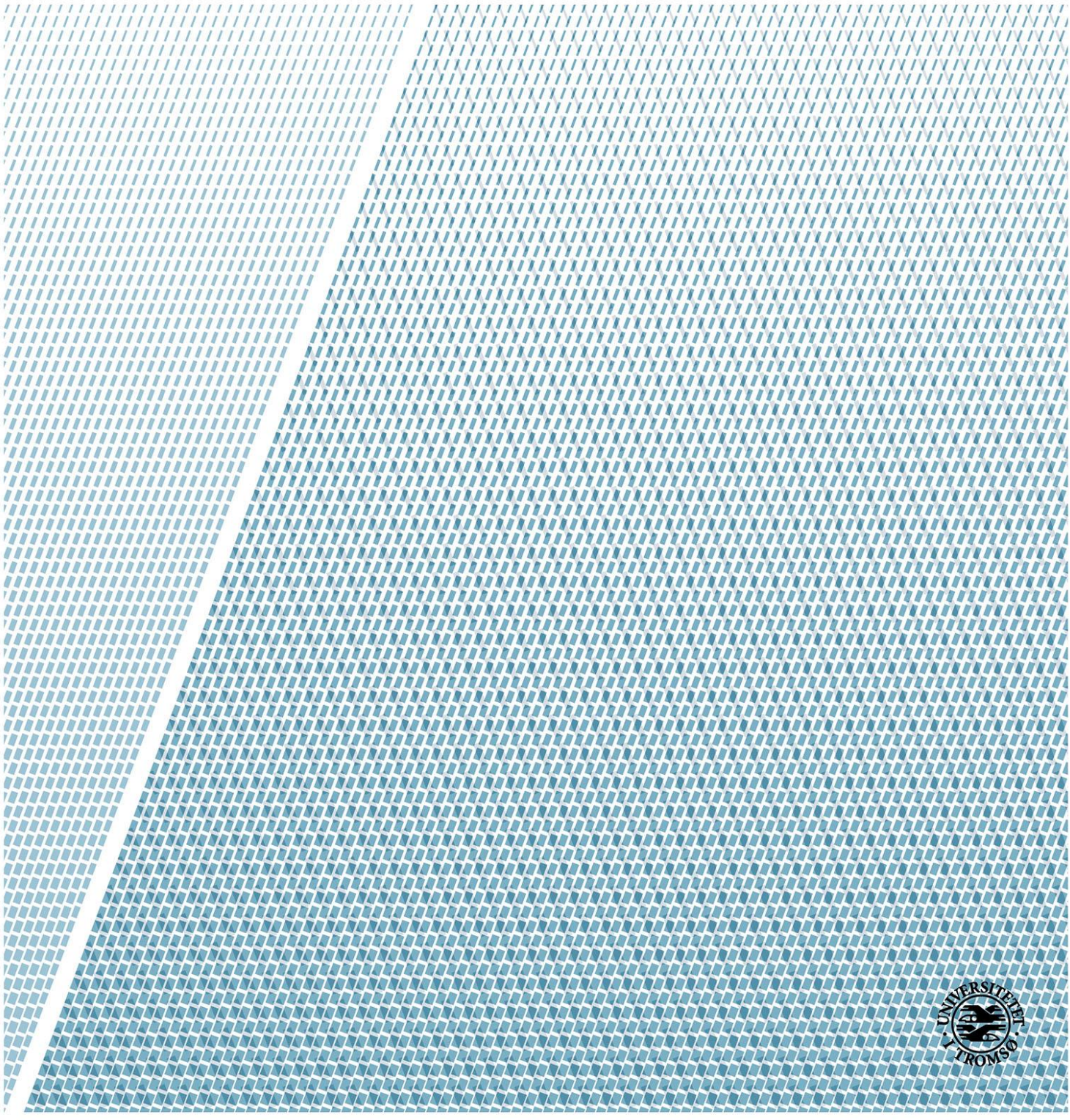

Preface

This thesis is the completion of my master's degree in Technology and Safety in the High North at UiT – the Arctic University of Norway, Tromsø, Norway. The work described in this report was carried out at the Department of Engineering and Safety in 2016-17. It is the original and independent work of the author except where specially acknowledged in the text. This thesis contains approximately 12504 words, 37 figures and 7 tables.

Odd Einar Lockertsen Myrli
Department of Engineering and Safety
UiT – the Arctic University of Norway
June 2017

Acknowledgement

I would like to thank my supervisor, Dr. Hassan A. Khawaja for his guidance throughout the work on the simulations. I would also like to thank the members of my study group; Sondre Ludvigsen, Cathrine H. Strand and Simon K. Skaga, for encouraging professional discussions during the two years of studying.

Odd Einar Lockertsen Myrli
Department of Engineering and Safety
UiT – the Arctic University of Norway
June 2017

Abstract

The number of good sites in less exposed locations for aquaculture farming is limited. Trends are now that the fish cages are increasing in both width and depth as well as more weather-exposed locations are taken into use. As the net cages continues to increase in size, so does the material costs. The design of the sea cages should be modified for safe and reliable use in remote offshore locations. Fish farms located in more exposed areas will be subject to more energetic waves and stronger currents, which will cause large net deformations. This is a challenge as fish welfare depends on a certain minimum volume within the net cage. Changing and maintaining net cages are some of the main expenses for fish farms. If the life time of the net cages are extended by introducing stronger, longer lasting materials, the overall costs of the nets would be reduced.

The traditional nets are produced in nylon, while the promising solid PET-wire has been introduced to the aquaculture industry. In this paper, we introduce polyurethane to the aquaculture net cages, which will be studied together with nylon and PET-wire. The study is carried out using fluid-structure interaction (FSI) simulation, which is coupling of fluid dynamics (CFD) and structure mechanics (FEM). ANSYS® software is employed in the study. We will look at the materials that shows the most promising results for aquaculture purposes.

List of content

List of figures

List of tables

Nomenclature

Symbols

S_n	--	Solidity ratio
σ_e	[Pa]	Equivalent stress
σ_1	[Pa]	Maximum principal stress
σ_2	[Pa]	Middle principal stress
σ_3	[Pa]	Minimum principal stress
F_s	--	Safety factor
S_{limit}	[Pa]	Specific stress limit where failure occurs if the maximum equivalent stress in the structure equals or exceeds this limit
$\mathbf{W}$	[kg]	Weight of the beam elements
$\mathbf{B}$	[N]	Buoyancy of the beam elements
ρ_m	[kg/m^3]	Material mass density
ρ_w	[kg/m^3]	Seawater density
g	[m/s^2]	Gravity
L_{total}	[m]	Total strand length of the rectangular net panel
d	[m]	Diameter of the beam elements
$A_{projected}$	[m^2]	Projected area of the beam elements
a_g	[m/s^2]	Global acceleration boundary condition for the net panel
M	[Nm]	Applied bending moment of the beam elements
E	[Pa]	Modulus of elasticity
I	[m^4]	Area moment of inertia of the beam cross section
κ	--	Resulting curvature of the beam
w_b	[m]	Deflection of the beam elements
x_b	[m]	Distance along the beam
σ_{axial}	[Pa]	Axial stress
F	[N]	Applied force on the beam elements
A	[m^2]	Cross-sectional area
δ	[m]	Deflection
L	[m]	Length of the beam element
τ	[Pa]	Shear stress of beam elements
V	[N]	Total shear force at the location
Q	[m^3]	Static moment of inertia
t_m	[m]	Thickness of the material perpendicular to the shear
$\boldsymbol{V}$	[m/s]	Velocity vector in Cartesian space
∇	--	Vector operator in Cartesian space
(x, y, z)	[m]	Spatial coordinates of some domain
t	[s]	Time
u	[m/s]	Velocity component in the x-direction
v	[m/s]	Velocity component in the y-direction

w	[m/s]	Velocity component in the z-direction
μ_M	[Pa·s]	Molecular viscosity coefficient
λ	[Pa·s]	Second viscosity coefficient
p	[Pa]	Pressure
(f_x, f_y, f_z)	[N]	Body force per unit mass acting on the fluid element
k	[J/kg]	Turbulent kinetic energy
ε	[J/(kg·s)]	Dissipation rate
G_k	[kg/(m·s^3)]	Generation of turbulence kinetic energy due to the mean velocity gradients
G_b	[kg/(m·s^3)]	Generation of turbulence kinetic energy due to buoyancy
Y_M	[kg/(m·s^3)]	Contribution of the fluctuating dilatation in compressible turbulence to the overall dissipation rate
$(C_2, C_{1\varepsilon}, C_{3\varepsilon})$	--	Constants in the epsilon equation
μ	[Pa·s]	Viscosity of the fluid
μ_t	[Pa·s]	Eddy viscosity
σ_k	--	Turbulent Prandtl number for the k equation
σ_ε	--	Turbulent Prandtl number for the epsilon equation
S_k and S_ε	--	User-defined source terms in the modelled transport equations for the realizable k-epsilon model
u_j	[m/s]	Average velocity component
S	--	Modulus of the mean rate-of-strain tensor
$\boldsymbol{F}_D$	[N]	Drag force
$\boldsymbol{F}_I$	[N]	Inertia force
C_D	--	Drag coefficient
A_{ref}	[m^2]	Reference area
$\boldsymbol{U}_R$	[m/s]	Relative flow velocity
C_a	--	Added mass coefficient
V	[m^3]	Body volume
U	[m/s]	Flow velocity
$\boldsymbol{V}_B$	[m/s]	Body velocity
$SG_{material}$	--	Specific gravity of the material

Abbreviations

CFD	Computational fluid dynamics
FEA	Finite element analysis
FEM	Finite element method
FSI	Fluid-structure interaction
PA	Polyamide (nylon)
PET	Polyethylene terephthalate

Definitions

Diadromous species
Diadromous fishes can both live in freshwater and in saltwater.

Floating collar
The frame which provides buoyancy and attachment for the net cages.

Fouling of the net
Fouling increases the weight of the net and decreases the water flow in and out of the net cage. Antifouling and/or frequent cleaning will prevent the fouling from building up, but you must still include a volume of fouling when dimensioning the net (see assumptions).

Mooring
Mooring is the system of lines and bottom attachments for keeping the floating collar in the desired position.

Fluid-structure interface
The solid surfaces of the net panel act as interfaces between the fluid and the solid domains, providing the means to transfer the pressure load from ANSYS Fluent to Structural mechanical.

Realizable k-epsilon model
The realizable model “means that the model satisfies certain mathematical constraints on the Reynolds stresses, consistent with the physics of turbulent flows.” [1]

Mesh and mesh shapes

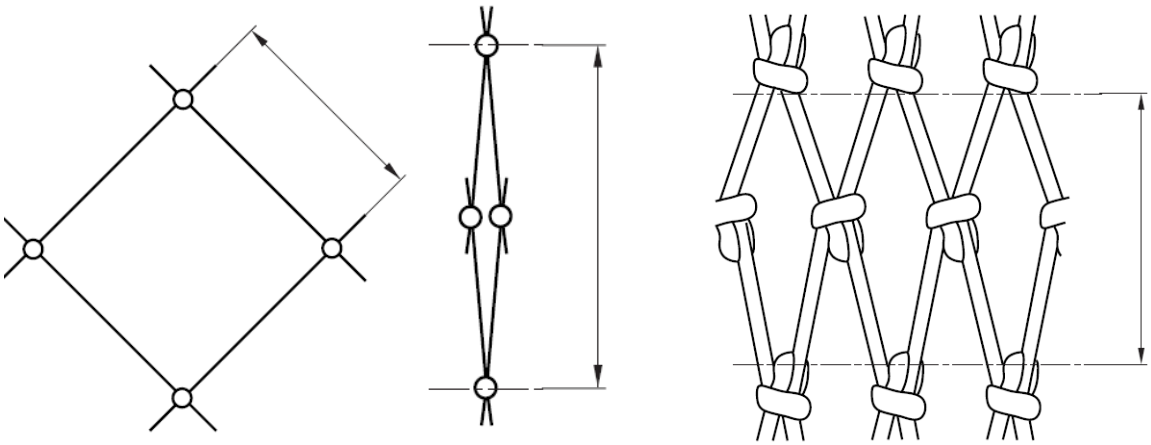

Figure 1 — Length of mesh side Figure 2 — Length of mesh Figure 3 — Opening of mesh

Figure 1 - Mesh and mesh shapes. [2]

Assumptions

- In this paper, the fish cage is not dimensioned to support a specific type of fish breed, as there are limitations in terms of water quality and temperatures for each breed. An analysis of environmental impact and conditions of the site must be performed before selecting the dimensions of the fish farms.

- When dimensioning the net, one should take the mutual influence between the main components, such as the floating collar and net cage, the net cage and mooring, etc. [3] p.33. As we are mainly looking at the materials of the net, the influences mentioned above have been neglected in the ANSYS® simulation. We are only looking at the nets used in aquaculture farms.

- The twine thickness is set to 4,5 mm (3mm + 50 % fouling) [4]. Several other aquaculture suppliers (together with Maccaferri KikkoNet) states that the twine thickness is 2-3 mm. Then, we must add a volume of fouling: "The calculations of the net pen shall at a minimum include a volume of fouling which gives up to 50 % increase of the twine diameter in the net pen as a whole." [5] p.45.

- The toxicity of the materials has not been considered in this thesis. The toxicity affects both the fish welfare as well as the marine ecosystem.

- In this paper, we assume that the fish farm is in an area with negligible shipping traffic to avoid the creation of waves from boats.

- The environmental temperature is set to 2,8°C, which is the lowest recorded seawater temperature in Tromsø according to seatemperature.org [6].

- We assume constant density and pressure for the water domain.

1. Introduction

"Cage aquaculture may date back to as early as the 1200s in some areas of Asia, and is currently a major form of aquaculture in countries including Canada, Chile, Japan, Norway and Scotland, where it has been used mainly for salmonid farming. However, a large variety of species are grown in cages today and include seawater, freshwater and diadromous species. Today, therefore, cages are used worldwide in the sea, in lakes and large rivers." [7] p.249. The number of good sites in less exposed locations for aquaculture farming are limited. Trends are now that the fish cages are increasing in both width and depth as well as more weather-exposed locations are taken into use. The design of the sea cages should be modified for safe and reliable use in more remote offshore locations. Fish farms located in more exposed areas will be subject to more energetic waves and stronger currents, which will cause large net deformations. This is a challenge as fish welfare depends on a certain minimum volume within the net cage.

"The introduction of the Norwegian standard NS 9415 in 2003 resulted in legal requirements for strength analysis of fish farms. Up until then, all net cages had been dimensioned using trade standards based on empirical data. NS 9415 requires strength analysis to validate the dimensioning of large net cages and net cages subjected to large environmental loads." [8] p.180-181. As simulation programs for finite element methods are advancing, the engineering analysis of the nets can contribute to improve the design, performance and reliability of the net cages. "An analysis involving a complete fluid and structure interaction model (CFD and FEA) will be complex and extremely demanding on computational resources, and to our knowledge attempts to perform such analysis on net cages have not been performed. There is ongoing work to verify and develop CFD methods for flow around net structures." [9] p.504.

"Modelling the hydrodynamic loads acting on a net cage is challenging due to hydroelasticity, i.e., fluid-structure interaction between moving sea-water and the flexible net." [8] p.181. The non-linear effects, detailed geometry and dynamic loads involved when analyzing a net cage makes it both complex and time consuming. Although computational power has increased immensely during the past decades, a full-scale analysis of aquaculture net cages using CFD methods is still unrealistic today, since the net consists of thousands of thin twines. The thin net twines make the water around the interface to divide down into many small elements by meshing in ANSYS Fluent (see figure 20).

"In open production units in the sea there will always be possibilities for fish escape as a result of construction failure. The weather is unpredictable and large waves can result in breakage of the production unit." [7] p.215. "The material strength of net panels exposed to sunlight (UV), wind, rain, acid rain, etc. is reduced. This process is called weathering." [7] p.263. To test the lifetime of the nets, you could implement a Xenon lamp aging test to see the elongation at break and time duration of the materials.

Figure 2 - Gloss surface of the mesh. [10]

"The lifetime of net cages can be increased by adding a colored (black) antioxidant, so the development of weathering is reduced. Today, however, white untreated material is commonly used for net bags." [7] p.263. "The normal life time of a net bag will vary with site conditions; in Norway, for example, the life time of a net bag is usually set as 5 years." [7] p.263. According to AkvaGroup®, the EcoNet PET-wire nets can stay in the water for up to 14 years. "This eliminates costly net changes and reduce the risk of net damage and fish escape during net handling." [11] p.37.

1.1 Offshore fish cages

The offshore fish cages can be floating, submerged or submersible. Where the nets used in the cages can be rigid or flexible. "Rigid nets may be created by using a flexible net attached to a stiff framework to distend it, or a rigid metal net that will maintain its original shape regardless of the waves." [7] p.249.

The most frequently used fish cage system in Norway is gravity cages that rely on buoyancy and weight to hold their shape and volume. [12] p.5.

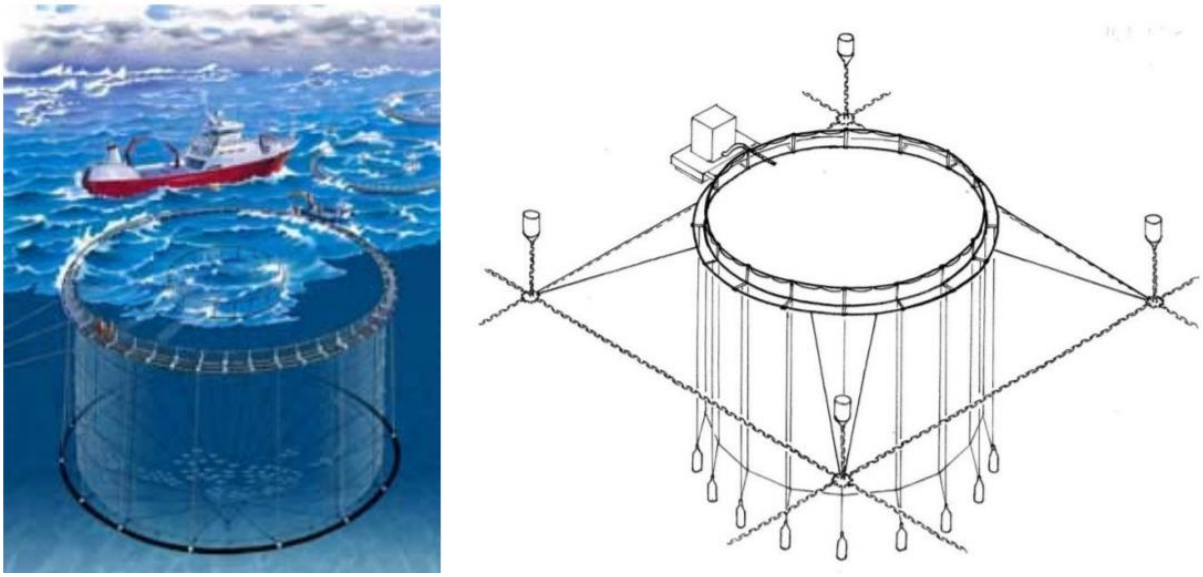

Figure 3 - Gravity cages. [12] p.5.

In this paper, the focus is on gravity cages, which are most used for intensive aquaculture. These cages usually consists of a mooring system, a jumping net to prevent fish escaping, a net cage with a plumb fixed directly or indirectly to the net cage to stretch the net, and a floating collar to provide buoyancy and attachment for the net cage. [7] p.250. The model used in the simulations consists of a net panel that refers to a section of the netting, with a force load to represent the separate weights in the bottom. The weights in the bottom maintain the shape of the net, either by separate weights or by a heavy bottom ring/sinker tube as you can see on the picture above.

1.1.1 Net cages

Net cages are built as a system of ropes and netting that can be constructed in various shapes, sizes and materials. The net cages are designed to transfer and carry all major forces through the ropes. The net cage is also supported by the mooring system that keeps the farm in a fixed position and to avoid transfer of excessive forces to the net cage. It is important to take account for the loads from current, waves, weights and handling of the net when dimensioning the net cage.

"In the past, materials such as cotton and flax were used for the net bags. These materials become heavy in water and their strength is rapidly reduced; in addition, they are not very durable. Nowadays, synthetic plastic materials such as polyamide (PA, nylon) predominate. This material is cheap, strong and not too stiff to work with." [7] p.262. The last decade, other materials like PET-wire (Polyethylene terephthalate) have been taken into use. PET-wire nets are semi-rigid, and requires less weights to keep the nets in place. The benefits of PET-wire are that it offers more protection against storm damage and predators like seals. Stronger materials also enable the net to better maintain its shape and may have a longer life span. This results in reduced deformation and drag, so the risk of rifts and other damage from adjacent equipment is reduced. PET-wire nets also have a reduced overall weight displacement for the cage system, which means less load on the mooring system and a reserve buoyancy for the cages. According to AkvaGroup®, the tensile strength of the EcoNet PET-wire is superior to Nylon and retains a high tensile strength for decades both below and above water. [13]

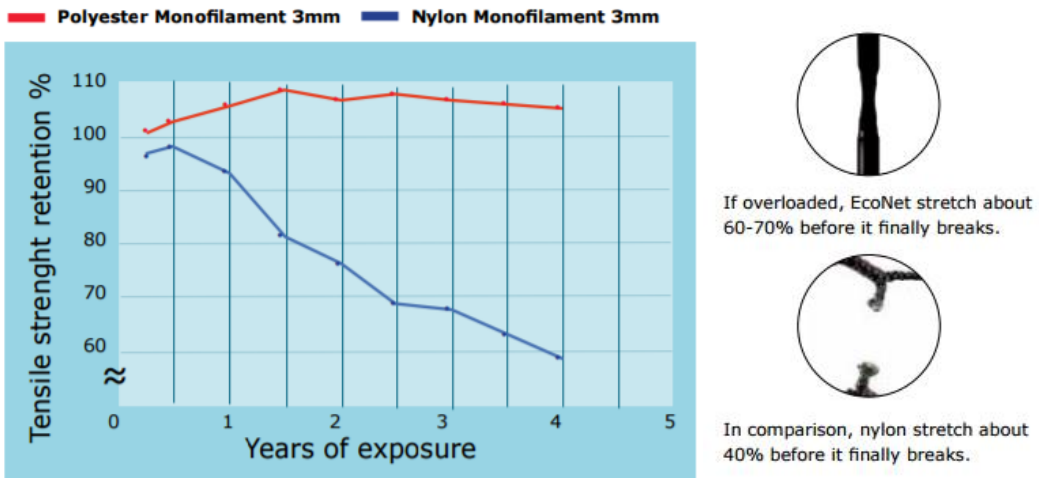

Figure 4 - Tensile strength retention of PET-wire and Nylon. [11] p.37,39.

However, the traditional nylon is a cheaper material, even though PET-wire may have a longer lifetime. PET-wire also weigh more, which can complicate the handling of large nets. Handling, together with other human errors and structural errors, are highlighted as some of the main challenges when it comes to fish escaping. [14] p.33.

In this thesis, polyurethane is also analyzed for use in net cages to compare with Nylon PA6 and PET-wire. China Institute of Water Resources & Hydropower Research in Beijing shows promising results for a material called the 'SK one component polyurea' (polyurethane base resin). They want to find new applications for the material together with UiT – the Arctic University of Norway. The advantages of polyurea are listed as the following [15] p.5.;

(1) good aging resistance;
(2) non-toxic;
(3) good anti-seepage and anti-abrasion performance;
(4) high strength, high elongation and good bonding with base concrete;
(5) good chemical resistance;
(6) good anti-freezing performance;
(7) simple and convenient construction.

The materials properties for the SK one component polyurea was analyzed by a fellow student, Hans-Kristian Norum Eidesen, at the University of Tromsø. The analysis was performed in a cold room at -30°C, so the results are not applicable for this project. That is why the material properties for the ester-based thermoplastic polyurethane was retrieved from RTP Company® as a guideline for what the behavior might look like [16]. To my knowledge, the material has not been tested for use in aquaculture net cages.

1.1.2 Changing and maintaining nets

"Net handling presents a major part of the total workload on a sea cage farm, and requires additional equipment."[7] p.391. Marine fouling is a problem for sea cages, and the degree of fouling can be reduced by having the mesh size as large as possible. "One or two sizes are typically used per year, but this depends on fish growth and species." [7] p.391. On more fouling-exposed sites, the nets may have to be changed more frequently. Changing the nets is heavy work and may require cranes to safely lift the nets during harvesting and cleaning to prevent rifts and other failures that may lead to escape. Netting of stronger materials like PET-wire may stay in the water until it is damaged, and can remain intact if a single wire is cut. According to AkvaGroup, the mesh shape will still be relatively stable with little effects on the structural strength. You can also do maintenance work like cleaning or antifouling on PET-wire nets while submerged, which greatly reduces the risk of net damage because of net handling. [11]

The hydrodynamic loads acting on a net cage depends slightly on the solidity of the netting material. "The solidity ratio (S_n) is used to describe how 'tight' a net is and is defined as the ratio between the area covered by the twines in the net and the total area of the net." [7] p.262.

$$S_n = 2 \cdot \frac{Twine\ diameter}{Length\ of\ mesh\ side} \quad or \quad \frac{Twine\ area}{Total\ area} \tag{1}$$

This relation is important when we want to find the resistance against the water flow through and around the net, which again determines the hydrodynamic loads acting on the cage. The solidity will increase because of fouling on the net, which leads to an increase in the covered area and reduces the oxygen supply for the fish. Algae growth can also increase bacterial loads and cause diseases and stress. The marine fouling can be removed by using filtered high-pressure seawater.

1.2 Structure of the report

In this thesis, I analyze the responses of the net panel subject to the environmental conditions, described by the displacements and the stresses, through analytical/numerical predictions and fluid-structure interaction simulation. The following points are focused on in this study:

- Literature review of fluid-structure interaction modelling of net cages. How the research with the finite elements analysis of net cages progresses, and how to model the behavior of nets subject to environmental loads.

- The methodology of how the study progresses from my preliminary study to how it was solved using FSI simulation, and some of the challenges I faced during the work on my simulations.

- Results and discussion of the fluid-structure interaction analysis for the various materials.

- Conclusion that sums up the discussion of this report.

- Future work, which highlights my thoughts on what ideas that could be initiated based on this study.

2. Literature review

"Research into the mechanical performance of nets has a long history. It progresses along two major lines: experimental studies (sometimes combined with in-situ observations) and analytical/numerical predictions." [17] p.251. Usually, aquaculture suppliers like Aqualine® use a combination of both, where they build a prototype and place it in a water pool that generates waves for the final testing. (Jørn Vidar Jakobsen, Aqualine Manager Northern Norway, personal communication, October 8, 2016)

2.1 Fluid-structure interaction analysis of nets

A fluid-structure interaction (FSI) simulation is a coupled fluid dynamics (CFD) and structure mechanics (FEM) case where we want to see how the fluid flow exerts the hydrodynamic forces on the net. The fluid flow calculates and pass flow fields from the CFD to the FEM code. The fluid elements in the fluid flow field will each undergo three different effects; translation, deformation and rotation. The hydrodynamic forces exerted on the net will deform and/or translate the net before the deformed/translated net imparts the velocity to the fluid domain and changes its shape, as well as the fluid flow. In a FSI analysis we study the interaction between two different physics phenomena, done in separate analyses/solvers. There are different modes of FSI modeling; rigid body FSI, one-way FSI and two-way FSI. With the rigid body FSI, we assume that there is no deformation in the solid structure and only the motions of the structure in the fluid are considered. This can be done in ANSYS Fluent alone, but it is not applicable for this project as we want to analyze the deformation for the net panel to compare the materials used. Two-way FSI is done in an iterative loop, i.e. the results of the CFD analysis at the fluid-structure interface are transferred to the mechanical model and applied as loads. Within the same analysis, the subsequently calculated displacements at the fluid-structure interface are mapped back to the CFD analysis. The loop continues until convergence is found, and often involves the changes to the mesh of the model. As we are working with thin twines that divides the water around the interface down into small elements, a two-way FSI will be too demanding for the computational resources with several twines. So, the one-way FSI mode is used for this study. [18]

In ANSYS, we can choose between two solvers for a fluid-structure interaction analysis. The CFX solver uses an element-based finite volume method, while Fluent uses the standard finite volume method and cell-centered solution to discretize the domain. The Fluent solver is used in this paper, as it may obtain better accuracy due to the increased number of data points compared to CFX that uses cell vertex numerics. Fluent allows us to import variables like temperature or pressure, in this case, from the cell or face zones in the Fluent solver to the structural finite element analysis. The ANSYS custom system Fluid Flow (Fluent) -> Static Structural (see figure below) is used for the one-way transfer FSI analysis. The system had to be modified, as the custom system you see at the top did not import the pressure. One-way FSI can also be done by system coupling.

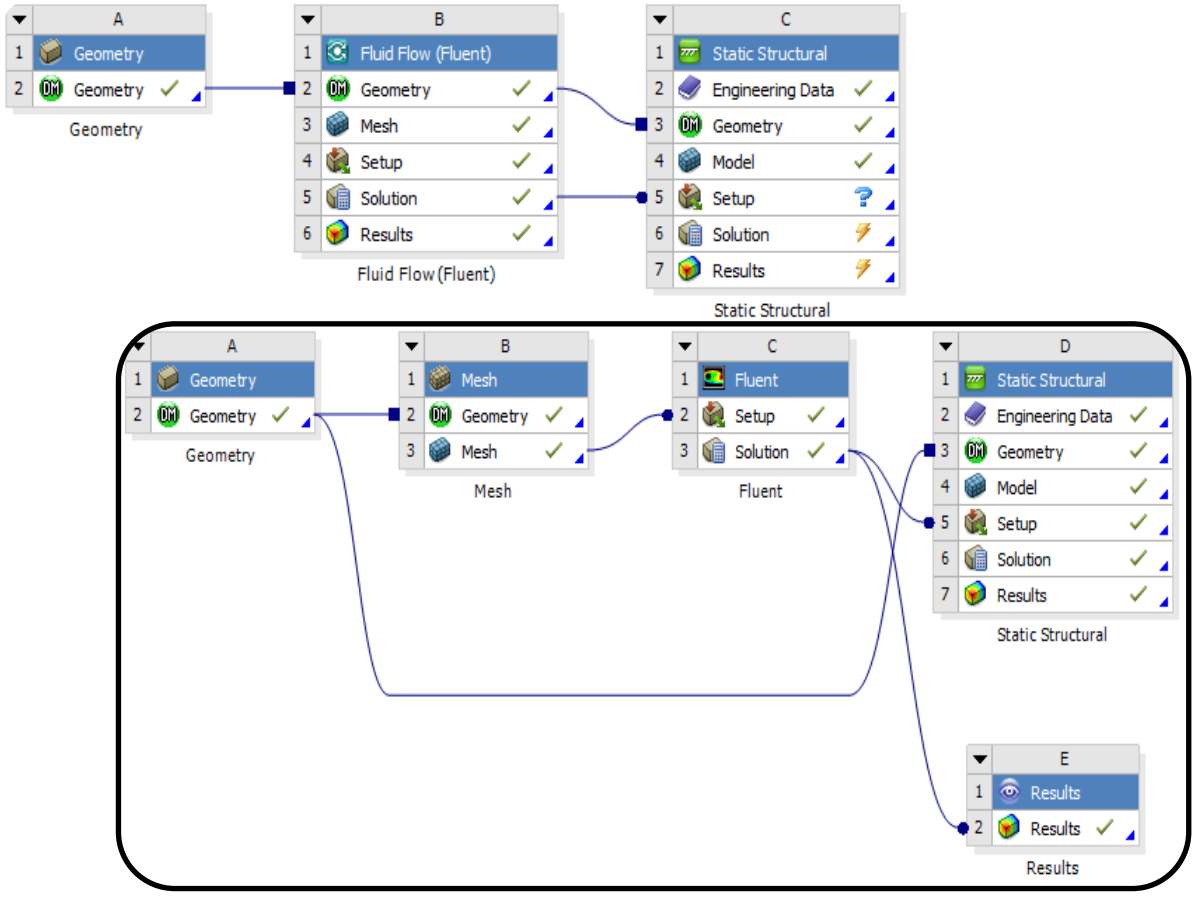

Figure 5 - FSI systems used in ANSYS Workbench.

In the custom FSI system, the CFD results are imported to the structural solver as a pressure load applied on the fluid-structure interface presented in figure 25. In a one-way FSI, the subsequently calculated displacements at the interface are not transferred back to the CFD analysis. The two models do not rely on matching meshes or include any modification of the meshes. The force applied at the interface allows us to investigate the hydrodynamic effects seawater have on the net panel.

2.1.1 Finite element modelling

A basic idea of the finite element method (FEM) is to divide a complex structure down into finitely small and geometrically simple bodies, called elements. These elements will in some sense model the behavior of the structure. Then we can describe the behavior of physical quantities at each element, and solve the system of equations at the nodes between each element. (FEM Book given as curriculum in TEK-3015 Multiphysics Simulation at UiT – the Arctic University of Norway by Hassan A. Khawaja, 2015) p.2.

In mechanical, the stress solutions allow us to predict the safety factors, stresses and displacements of the net panel and compare the results for the various materials. The ANSYS yield criterion is based on the Von Mises equivalent stress, which is given as;

$$\sigma_e = \sqrt{\frac{1}{2}[(\sigma_1 - \sigma_2)^2 + (\sigma_2 - \sigma_3)^2 + (\sigma_3 - \sigma_1)^2]} \quad (2)$$

Where σ_e is called the equivalent stress, while σ_1, σ_2 and σ_3 are referred to as the principal stresses. In mechanical, the principal stresses are always ordered such that σ_1 is the maximum, σ_2 is the middle and σ_3 is the minimum stress. The yield occurs when the Von Mises equivalent stress exceeds the uniaxial material yield strength. The safety factor is;

$$F_s = \frac{S_{limit}}{\sigma_e} \tag{3}$$

where S_{limit} is the specific stress limit where failure occurs if the maximum equivalent stress in the structure equals or exceeds this limit. [19] p.883, 906.

2.1.1.1 Forces acting on the beam elements

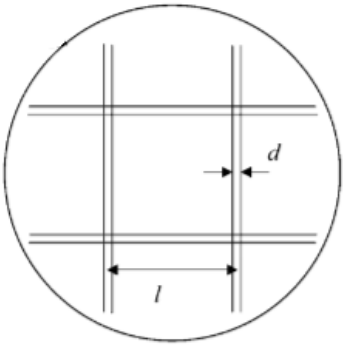

Figure 6 - Net mesh geometry. [17] p.255.

The weight, buoyancy and projected area of each of the beam elements are:

$$\boldsymbol{W} = \pi \boldsymbol{g} \rho_m L_{total} \frac{d^2}{4} \tag{4}$$

$$\boldsymbol{B} = \pi \boldsymbol{g} (\rho_w - \rho_m) L_{total} \frac{d^2}{4} \tag{5}$$

$$A_{projected} = L_{total} \cdot d \tag{6}$$

Where ρ_m is the material mass density, ρ_w is the seawater density, g is the gravity, d is the diameter of the beam element and L_{total} is the total strand length of the rectangular net panel. [17] p.256.

The global acceleration boundary condition for the net panel is calculated by the buoyancy of the net and the gravity.

$$a_g = \frac{\rho_{material} - \rho_{water}}{\rho_{water}} \cdot g \tag{7}$$

The bending stiffness of the beam elements is a function of the modulus of elasticity and the area moment of inertia:

$$M = EI\kappa = EI \frac{\partial^2 w_b}{\partial {x_b}^2} \tag{8}$$

Where M is the applied bending moment, w_b is the deflection of the beam and x_b is the distance along the beam. E is the modulus of elasticity, where small values means a flexible material and large values indicate rigid material. I is the area moment of inertia of the beam cross section. [20] p.6-7.

S.B.A. Invent [21] defines the axial stress and the deflection of beam elements.
The axial stress is defined as:

$$\sigma_{axial} = \frac{F}{A} \tag{9}$$

Where F is the applied force and A is the cross-sectional area resisting the load.
"Typically, the stress on a part under axial loading is constant when the cross-sectional area is constant. However, at the fixed point it can be seen that the stress can vary. This is known as Saint Venant's Principle, and can only be seen through Finite Element Analysis." [21]

The deflection δ is defined as:

$$\delta = \frac{FL}{AE} \tag{10}$$

Where F is the applied force, L is the length of the beam element, A is the cross-sectional area resisting the load and E is the modulus of elasticity.

The formula to calculate the shear stress of beams is defined "as the internal shear stress of a beam caused by the shear force applied to the beam." [22]

$$\tau = \frac{VQ}{It_m} \tag{11}$$

Where V is the total shear force at the location, Q is the static moment of area, I is the moment of inertia of the entire cross-sectional area and t_m is the thickness in the material perpendicular to the shear.

2.1.2 Computational fluid dynamics

Computational fluid dynamics (CFD) is a design tool for fluid dynamics and aerodynamics. CFD was developed in the 1960s by military research with the needs of the aerospace community. The central basis of CFD is a) mass is conserved, b) conservation of momentum (Newton's second law, $F = ma$) and c) energy is conserved. When solving fluid-structure interaction problems, the CFD solver uses the Navier-Stokes equations to import the pressure from the fluid domain over to the structural domain.

Navier-Stokes equations are a set of coupled differential equations that "consists of a time-dependent continuity equation for conservation of mass, three time-dependent conservation of momentum equations and a time-dependent conservation of energy equation." [23] High-speed computers can solve approximations to the equations by using a variety of techniques like the finite difference, finite volume, finite element and spectral methods. Only the continuity equation and the momentum equation are presented, as the energy equation for analyzing thermal conditions is disabled for this problem.

The continuity equation in conservation form, from [24] p. 55;

$$\frac{\partial \rho}{\partial t} + \left[\frac{\partial(\rho u)}{\partial x} + \frac{\partial(\rho v)}{\partial y} + \frac{\partial(\rho w)}{\partial z}\right] = 0 \tag{12.1}$$

$$\frac{\partial \rho}{\partial t} + \nabla \cdot (\rho \boldsymbol{V}) = 0 \tag{12.2}$$

The momentum equation in conservation form, from [24] p.66;
x-momentum:

$$\frac{\partial(\rho u)}{\partial t}+\frac{\partial(\rho u^2)}{\partial x}+\frac{\partial(\rho uv)}{\partial y}+\frac{\partial(\rho uw)}{\partial z}=-\frac{\partial p}{\partial x}+\frac{\partial}{\partial x}\left(\lambda\nabla\cdot\boldsymbol{V}+2\mu_M\frac{\partial u}{\partial x}\right)+\frac{\partial}{\partial y}\left[\mu_M\left(\frac{\partial v}{\partial x}+\frac{\partial u}{\partial y}\right)\right]+\frac{\partial}{\partial z}\left[\mu_M\left(\frac{\partial u}{\partial z}+\frac{\partial w}{\partial x}\right)\right]+\rho f_x \quad (13)$$

y-momentum:

$$\frac{\partial(\rho v)}{\partial t}+\frac{\partial(\rho uv)}{\partial x}+\frac{\partial(\rho v^2)}{\partial y}+\frac{\partial(\rho vw)}{\partial z}=-\frac{\partial p}{\partial y}+\frac{\partial}{\partial x}\left[\mu_M\left(\frac{\partial v}{\partial x}+\frac{\partial u}{\partial y}\right)\right]+\frac{\partial}{\partial y}\left(\lambda\nabla\cdot\boldsymbol{V}+2\mu_M\frac{\partial v}{\partial y}\right)+\frac{\partial}{\partial z}\left[\mu_M\left(\frac{\partial w}{\partial y}+\frac{\partial v}{\partial z}\right)\right]+\rho f_y \quad (14)$$

z-momentum:

$$\frac{\partial(\rho w)}{\partial t}+\frac{\partial(\rho uw)}{\partial x}+\frac{\partial(\rho vw)}{\partial y}+\frac{\partial(\rho w^2)}{\partial z}=-\frac{\partial p}{\partial z}+\frac{\partial}{\partial x}\left[\mu_M\left(\frac{\partial u}{\partial z}+\frac{\partial w}{\partial x}\right)\right]+\frac{\partial}{\partial y}\left[\mu_M\left(\frac{\partial w}{\partial y}+\frac{\partial v}{\partial z}\right)\right]+\frac{\partial}{\partial z}\left(\lambda\nabla\cdot\boldsymbol{V}+2\mu_M\frac{\partial w}{\partial z}\right)+\rho f_z \quad (15)$$

The equations are in a partial differential form, derived based on an infinitesimally small element fixed in space. The term inside the brackets of the continuity equation (12.1) is simplified to $\nabla\cdot(\rho\boldsymbol{V})$ where ρ is the density, and "$\nabla\cdot\boldsymbol{V}$ is called the convective derivative, which is physically the time rate of change due to the movement of the fluid element from one location to another in the flow field where the flow properties are spatially different." [24] p.45. The velocity vector in Cartesian space is given by;

$$\boldsymbol{V}=u\boldsymbol{i}+v\boldsymbol{j}+w\boldsymbol{k} \quad (16)$$

while the vector operator in Cartesian coordinates is defined as;

$$\nabla=\boldsymbol{i}\frac{\partial}{\partial x}+\boldsymbol{j}\frac{\partial}{\partial y}+\boldsymbol{k}\frac{\partial}{\partial z} \quad (17)$$

"There are four independent variables in the problem, the x, y, and z spatial coordinates of some domain, and the time t. …three components of the velocity vector; the u component is in the x direction, the v component is in the y direction, and the w component is in the z direction." [23]

For the momentum equation, we assume the fluid to be Newtonian. "Isaac Newton stated that shear stress in a fluid is proportional to the time rate of strain, i.e., velocity gradients." [24] p.65. Then μ_M is the molecular viscosity coefficient and λ is the second viscosity coefficient. "Stokes made the hypothesis that

$$\lambda=-\frac{2}{3}\mu_M \quad (18)$$

which is frequently used but which has still not been definitely confirmed to the present day." [24] p.66. Finally, we have the pressure p and the body force per unit mass acting on the fluid element f_x, f_y and f_z.

The modelled transport equations for the realizable k-epsilon model are presented by ANSYS Help Viewer [25]:

k equation:

$$\frac{\partial}{\partial t}(\rho k) + \frac{\partial}{\partial x_j}(\rho k u_j) = \frac{\partial}{\partial x_j}\left[\left(\mu + \frac{\mu_t}{\sigma_k}\right)\frac{\partial k}{\partial x_j}\right] + G_k + G_b - \rho\varepsilon - Y_M + S_k \quad (19)$$

Epsilon equation:

$$\frac{\partial}{\partial t}(\rho\varepsilon) + \frac{\partial}{\partial x_j}(\rho\varepsilon u_j) = \frac{\partial}{\partial x_j}\left[\left(\mu + \frac{\mu_t}{\sigma_\varepsilon}\right)\frac{\partial \varepsilon}{\partial x_j}\right] + \rho C_1 S\varepsilon - \rho C_2 \frac{\varepsilon^2}{k+\sqrt{\nu\varepsilon}} + C_{1\varepsilon}\frac{\varepsilon}{k}C_{3\varepsilon}G_b + S_\varepsilon \quad (20)$$

Where

$$C_1 = max\left[0.43, \frac{\eta}{\eta+5}\right], \eta = S\frac{k}{\varepsilon}, S = \sqrt{2S_{ij}S_{ij}}\ and\ S_{ij} = \frac{1}{2}\left(\frac{\partial u_j}{\partial x_i} + \frac{\partial u_i}{\partial x_j}\right)$$

"In these equations, t is time, ρ is the density of the fluid, k is the turbulent kinetic energy and ε is the dissipation rate. G_k represents the generation of turbulence kinetic energy due to the mean velocity gradients. G_b is the generation of turbulence kinetic energy due to buoyancy. Y_M represents the contribution of the fluctuating dilatation in compressible turbulence to the overall dissipation rate. C_2, $C_{1\varepsilon}$ and $C_{3\varepsilon}$ are constants. σ_k and σ_ε are the turbulent Prandtl numbers for k and ε, respectively. S_k and S_ε are user-defined source terms. μ is the viscosity of the fluid, while μ_t is the eddy viscosity. u_j is the average velocity component. S is the modulus of the mean rate-of-strain tensor." [25]

The continuity equation, momentum equations, k- and epsilon equation are the equations ANSYS Fluent solves as seen in figure 23.

2.2 Methods for modelling nets for aquaculture farms

"Today, load models for net cages are typically based on Morison's equation, 2D panel tow-tests and so-called screen models." [8] p.181.

I. Tsukrov, et al. [17] propose a consistent one-dimensional net element to be used in the finite element method to model the dynamic response of net panels to open ocean environmental loading. The net panel refers to a section of netting between supports, see picture below. Their focus is centered on the numerical modelling of deformation and overall dynamic behavior of nets subjected to wave and current loading. The simulations were done in the AQUA-FE program that is developed at the University of New Hampshire. This "is an advanced computer design and analysis tool to model the dynamic response of partially or completely submerged structures in an ocean environment." [17] p.260.

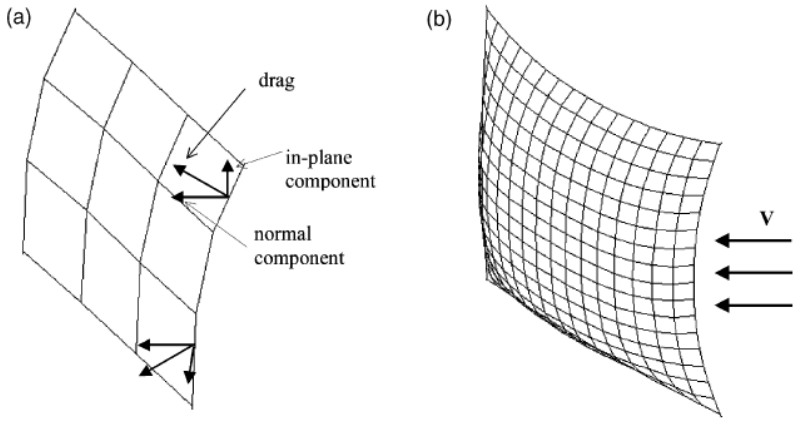

Figure 7 - Model of a net panel using a different number of elements for the same panel. (a) 24 elements; (b) 544 elements; V represents the direction of the fluid velocity. [17] p.264.

H. Moe, et al. [9] modelled a net cage using 3-D truss elements that represented several parallel twines. Sub-elements allowed the trusses to buckle in compression. "The truss elements were given the combined properties of the represented twines, i.e. the cross-section area of the truss element was equal to the sum of the cross- section area of the represented twines." [9] p.505. This thesis take inspiration from the combined twines into beam elements when modelling the net panel for the simulations. The paper from H. Moe et. al. presents "a method for numerical strength analysis of net cages in constant uniform current verified for limited solidity, deformations and current velocities, applying Morison's equation to calculate loads on the deformed net cage. …Strength analyses were performed using the finite element method software ABAQUS Explicit." [9] p.504-505. ABAQUS is similar to ANSYS when doing a finite element analysis.

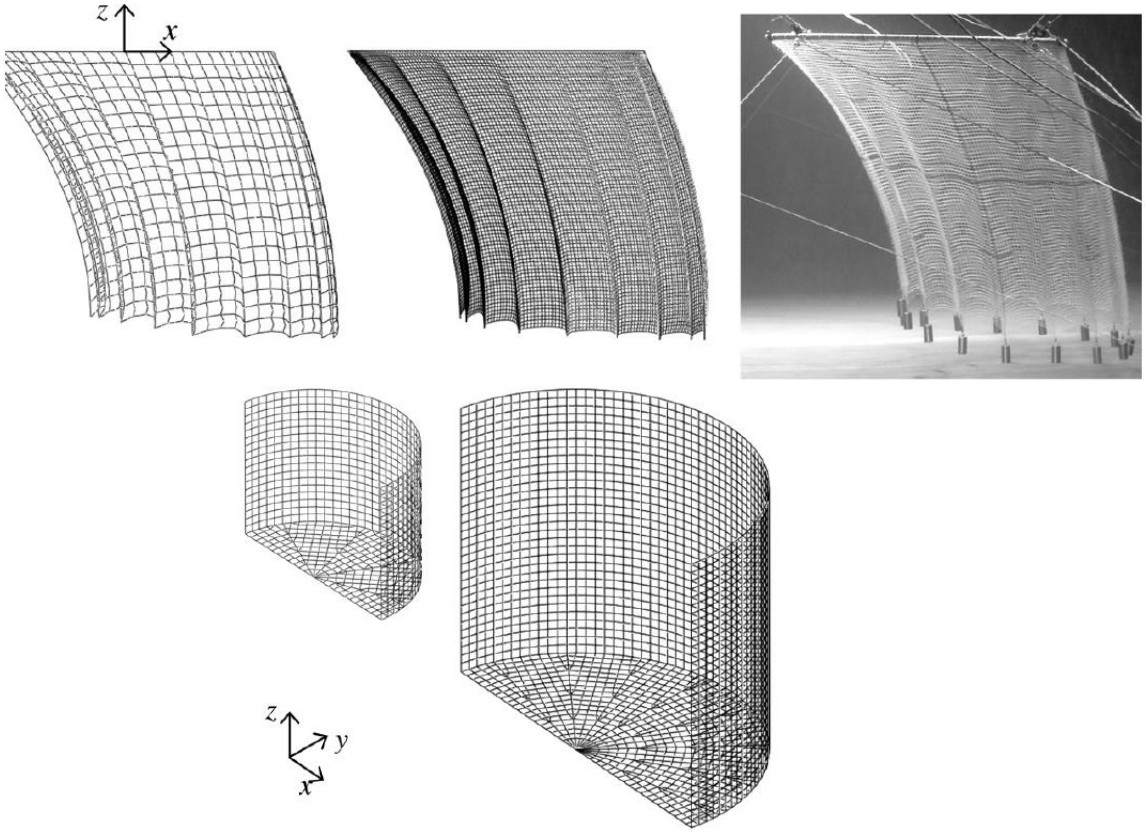

Figure 8 - The figures show the models H. Moe, et al. used for the simulations of the net cage. [9] p.505-506.

Another applied approach presented by Zhao, Y.-P., et al. [26] was to model the net as a porous medium. Here, the solidity of the net is decided by the porosity to make the structure affect the flow pattern in the fluid domain. The finite volume method was used to solve the governing equations of the numerical model using ANSYS Fluent 6.3.

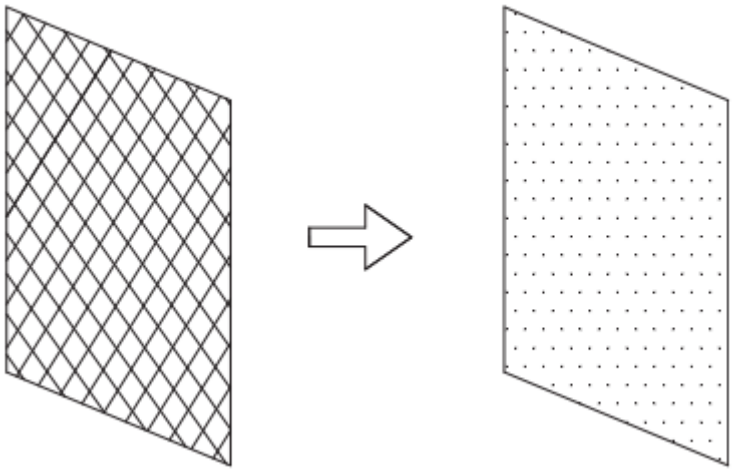

Figure 9 - Porous media model [26]. p.26.

2.3 Forces acting on a net cage

When dimensioning a net cage, the net should be constructed to reproduce the drag, buoyancy, inertial and elastic forces exerted on the netting by current and waves. "On ordinary sites it will be the current that causes the highest forces, while on more exposed sites the wave forces will be considerable." [7] p.274-275.

"The resulting forces on a moving body in an unsteady viscous flow can be determined using Morrison equation, which is a combination of an inertial term and a drag term:

$$\boldsymbol{F} = \boldsymbol{F}_D + \boldsymbol{F}_I \tag{21}$$

Where the drag force is given by:

$$\boldsymbol{F}_D = \frac{1}{2}\rho_w C_D A_{ref} \boldsymbol{U}_R |\boldsymbol{U}_R| \tag{22}$$

ρ_w is the water density, C_D is the drag coefficient, A_{ref} is the reference area and $\boldsymbol{U}_R = \boldsymbol{U} - \boldsymbol{V}_B$ is the relative flow velocity, **U** is the flow velocity and $\boldsymbol{V}_B$ is the body velocity.
And the inertia force is given by:

$$\boldsymbol{F}_I = \rho_w C_a V \dot{\boldsymbol{U}}_R + \rho_w V \dot{\boldsymbol{U}} \tag{23}$$

Where C_a is the added mass coefficient and V is the body volume. Bold letters denote vectors." [27] p.1003.

3. Methodology

This chapter discusses the methodology used to design the net panel and to study the materials used in fish cages. The study is carried out using ANSYS Workbench® version 18.1 on a Lenovo ThinkStation P910. The chapter gives a detailed overview of how the study progressed from my preliminary study to how it was solved in the mentioned simulation program.

3.1 Preliminary study

The preliminary study was carried out using ANSYS Workbench® version 17.1 and postprocessing in Autodesk 3ds Max®. The study was a purely mechanical (FEM) analysis of nylon PA6 and PET-wire; it did not include the hydrodynamic loads acting on the net cage. So, the only forces defined on the net was the weights and the fixed supports. Note that the material properties used in the preliminary study are not the same as for this thesis.

3.1.1 Modelling the net cage in 3ds Max

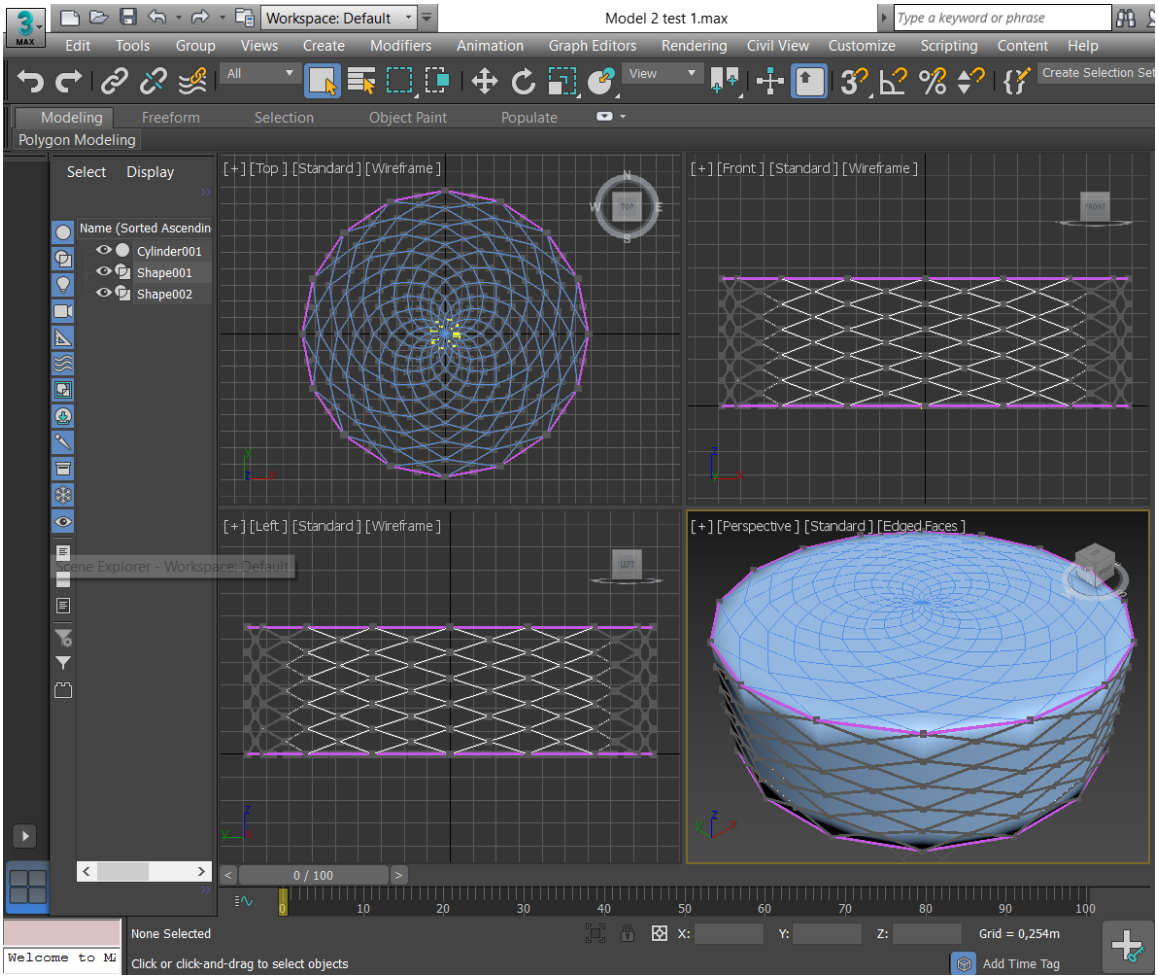

Figure 10 - One of my test models in 3ds Max. Inspiration from: [28].

The program is user-friendly with many different modifiers that makes the modelling process easier. With the editable poly function, a primitive object like a cylinder can be divided into sub-objects (in the form of polygons) that you can modify. With the editable poly function, you can build any model you can imagine, and this is the method I used to model the net cage.

Before importing the geometry file into ANSYS Workbench, the file must be saved as type: AutoCad (*.DWG). For an accurate export to ANSYS Workbench, the unit setup must be customized to metric meters in 3ds Max. The import to ANSYS only contained line bodies, as the surface bodies will make a volume inside the mesh twines (this is the blue shades between the twines as you can see in the figure above). So, over 8000 different parts were reduced to 38 parts when imported to ANSYS DesignModeler. After importing the CAD file to ANSYS workbench, I had to define the cross-section area for the twines, as line bodies do not have a surface area or volume. Finally, the parts were united into one body using the Boolean body operation in ANSYS Geometry.

Postprocessing in 3ds Max proved to be incompatible with ANSYS Fluent as the imported model did not have any faces, which are needed for selecting the fluid-structure interface and to subtract the solid body from the water. This problem may have been possible to solve within 3ds Max settings and/or by saving the file as another file type.

I described the bodies by the materials and the imported geometry in ANSYS workbench.

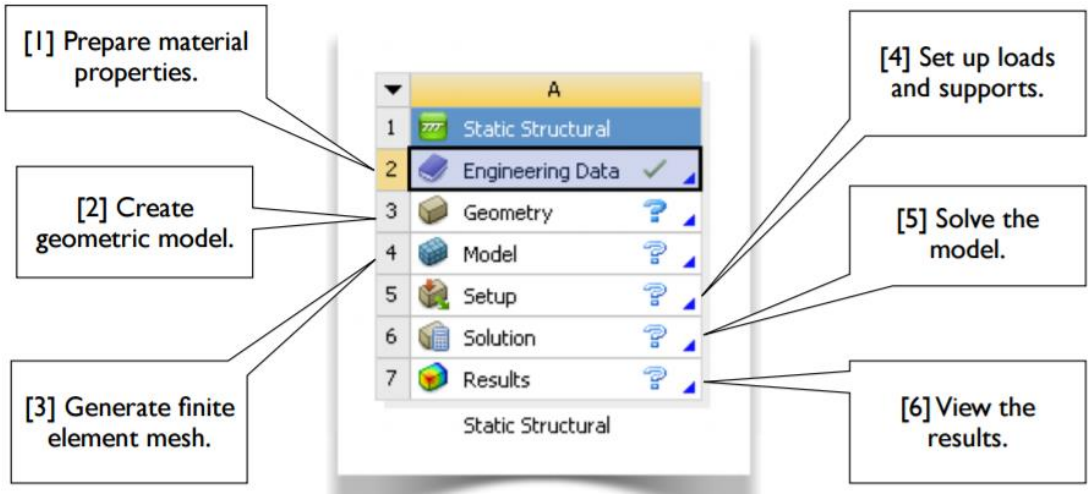

Figure 11 - Static Structural analysis in ANSYS Workbench® [29] p.4.

Transient structural analysis was used in ANSYS Workbench® for a dynamic analysis. The illustration above still describes the main elements when performing the simulation. In Engineering Data, the material properties are defined for each of the materials, with Young's Modulus, Poisson's ratio and density (which must be specified when inertia forces are involved e.g., dynamic simulations). As the net cage with a diamond shaped mesh is difficult to design in the built-in DesignModeler geometry, the geometric model was created in 3ds Max.

3.1.2 Finite element analysis of the net cage

By creating a mesh, we create a mesh of nodes, and the results are calculated by solving the governing equations numerically at each of the nodes using the finite element method.
In the preliminary study, a mechanical physics preference was used for the mesh which transformed the single body into 6737 nodes and 3584 elements. As the external flows around the net were yet to be modelled, a Lagrangian formulation is used. The Lagrangian

formulation is usually used for finite element analysis (FEA) of solids, and the nodes are associated with material points. [30] p.21.

The material properties used for the preliminary project are presented in table 1. The values differ from the material properties used in this paper, as obtained from RTP Company.

	Nylon PA6	**PET-wire**
Young's Modulus	2900 MPa	3000 MPa
Poisson's ratio	0,39	0,39
Density	1158,25 kg/m^3	1380 kg/m^3

Table 1 - Material properties for the preliminary project. Ref. PET-wire: [20] p.36. Ref. Nylon: [31] and [32].

The net cage was created with the following properties:

Diameter	4.48 m = 16x Truss length
Depth	1.40 m = 5x Truss length
Truss length	0.28 m
Twine thickness	3 mm+50% fouling = 0.0045 m
Truss thickness	4x Twine thickness = 0.018 m
Truss cross-section area	254.47 mm^2

Table 2 - Geometric properties of the net cage modelled in the preliminary study, with inspiration from Table 1, H. Moe, et al. [9] p.505.

The model was constraint by setting a fixed support in all vertexes on the top rope as you can see on the figure below. Then, the separate weights were set at the bottom rope as well as one in the middle. Each weight was set to be 800g with inspiration from H. Moe, et al. Model M1 [9] p.505.

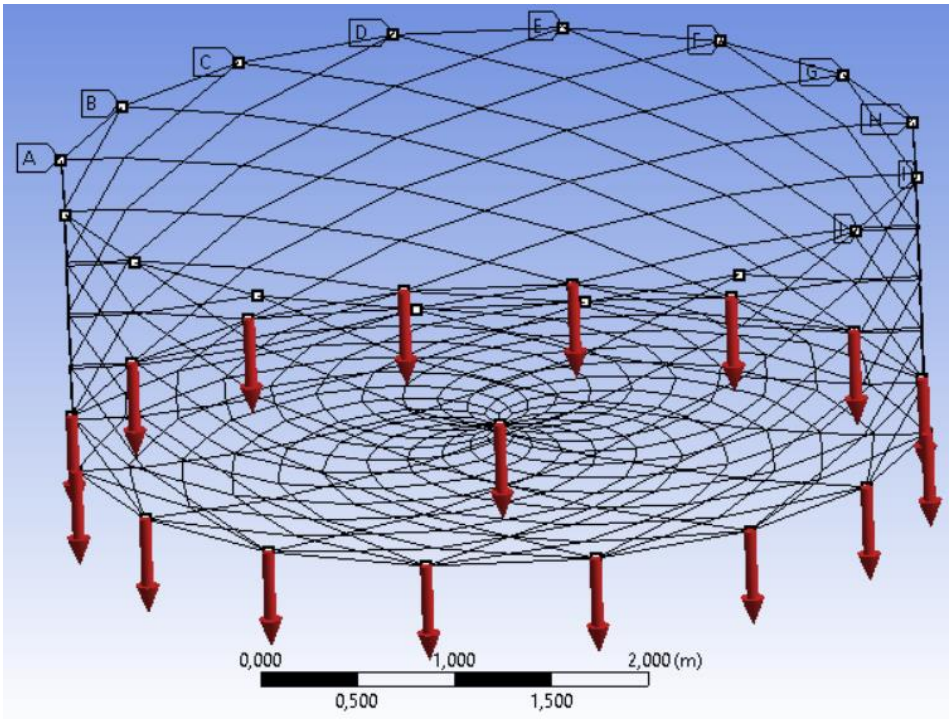

Figure 12 - Fixed supports at the top rope and separate weights at the bottom segment from the ANSYS simulation.

Next, the model was solved for both Nylon (PA6) and PET-wire, where the results is discussed below.

3.1.3 Results of the preliminary study

3.1.3.1 Total deformation of the net cage

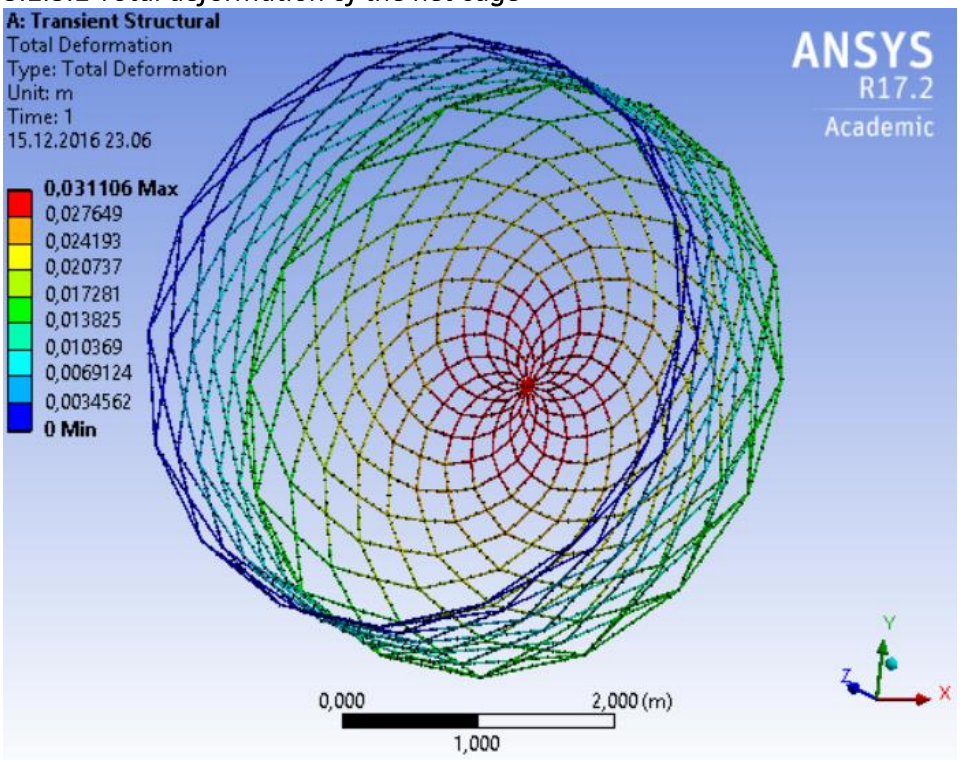

Figure 13 - Total deformation of the net with PET-wire.

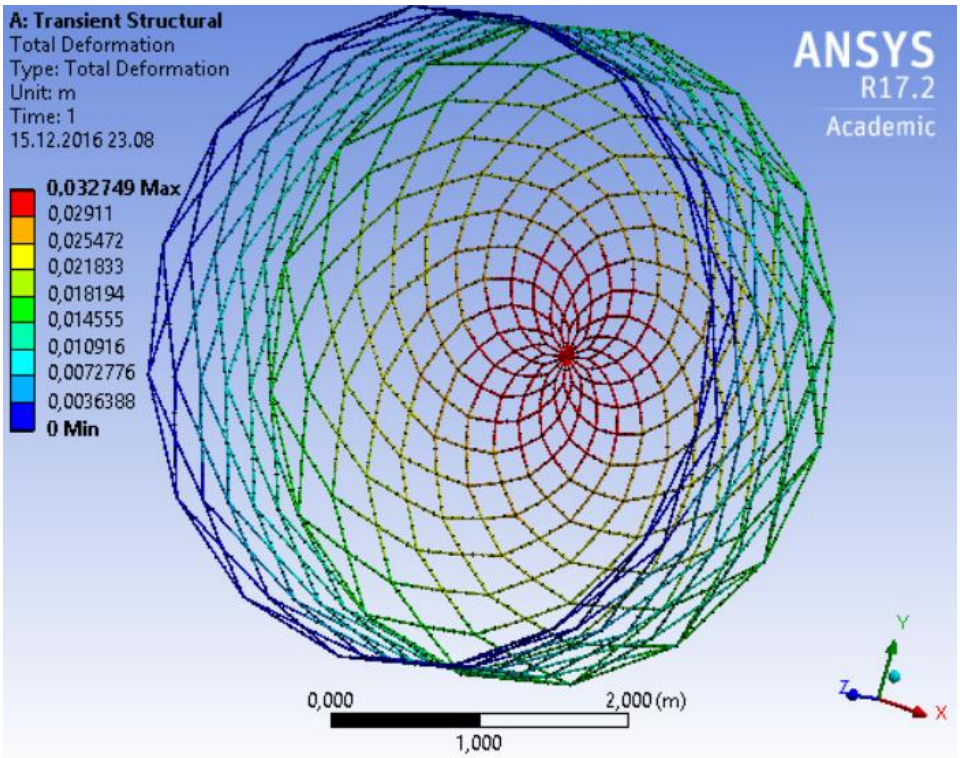

Figure 14 - Total deformation of the net with nylon PA6.

The deformation increases towards the center of the net cage. As mentioned in the introduction, stronger materials are better to maintain the shape of the net. The figures above confirm the theory, with a larger deformation for nylon, which is the lighter material.

3.1.3.2 Axial forces

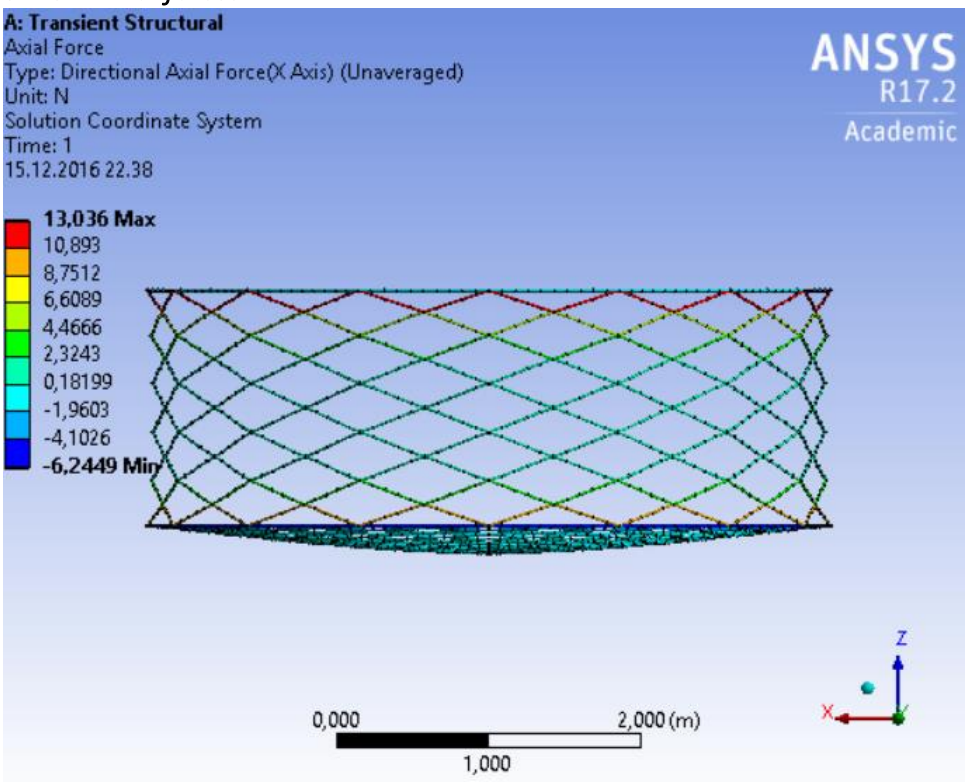

Figure 15 - Axial forces on the net with PET-wire.

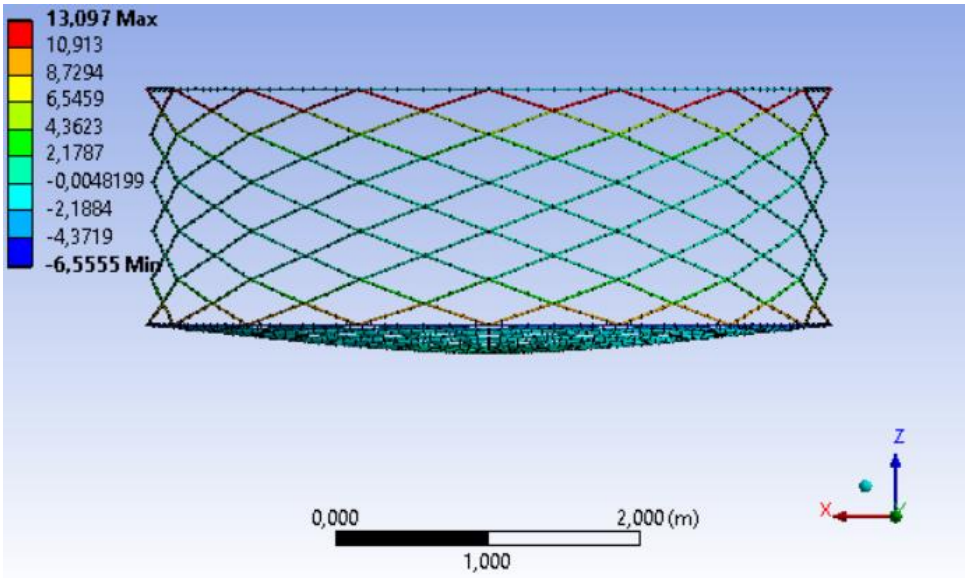

Figure 16 - Axial forces on the net with nylon PA6.

The axial forces are largest near the top and bottom ropes (marked in red and orange) which means we have the most tension here. This is because of the weights that was placed around the bottom segment. The maximum tension force is larger for nylon, and nylon also have the largest compression on the opposite side of the scale.

3.1.3.3 Total shear force

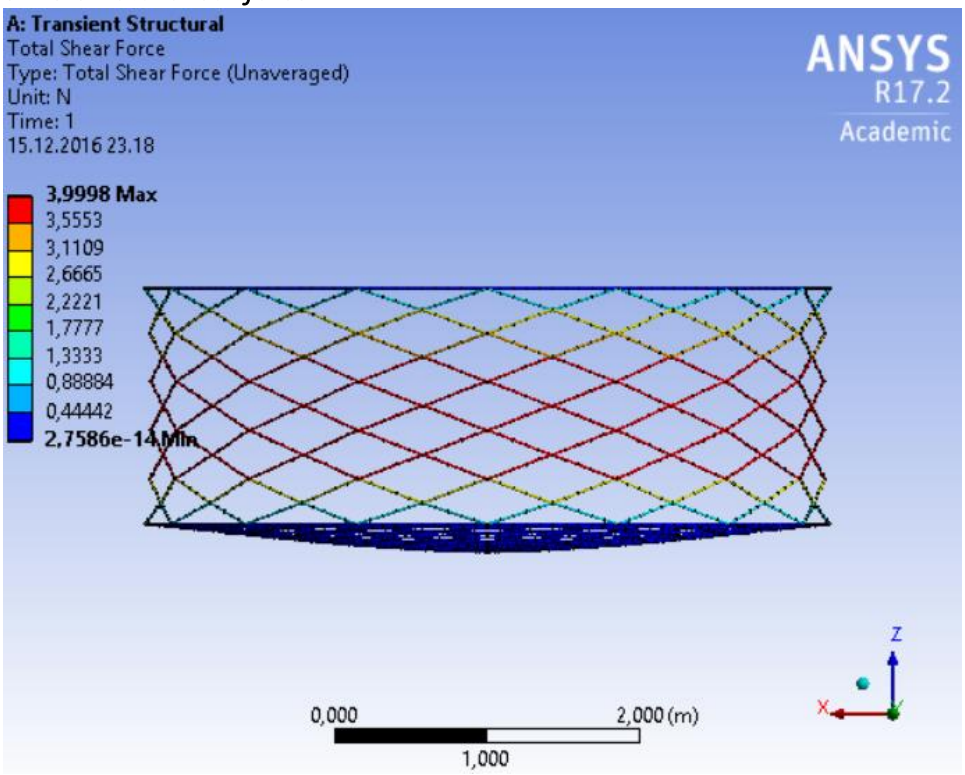

Figure 17 - Total shear force for the net with PET-wire.

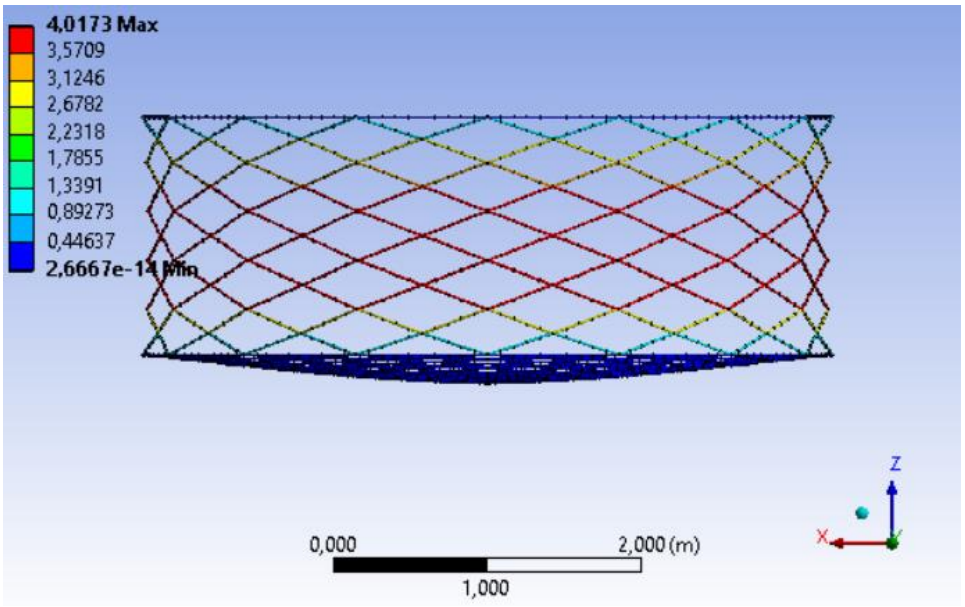

Figure 18 - Total shear force for the net with nylon PA6.

The total shear force is largest around the center of the net sides. The force was yet again largest for nylon PA6.

3.1.4 Conclusions from the preliminary study

Following conclusions were drawn from the preliminary study:

- PET-wire proved to be the strongest material, however, nylon PA6 is a cheaper option and the results did not differ enough to say that using PET-wire would pay off.

- The material properties chosen for the study are quite similar for the two materials, this is the reason why the results are so similar for both materials.

- The net should have been constructed to reproduce the drag, buoyancy, inertial and elastic forces exerted on the netting by current and waves. The fact that we are lacking the environmental loads from current and waves do not make the results comparable to the reality.

3.2 FSI in ANSYS Workbench

Following the preliminary study, new models are designed for the fluid-structure interaction analysis. The net is constructed to reproduce the hydrodynamic forces exerted on the netting by currents and waves. We describe the bodies by geometries and materials in ANSYS Workbench. The environmental conditions will include support and loading conditions, and the responses of the net panel subject to the environmental conditions are described by the displacements and the stresses.

3.2.1 Modelling circular net cages

Some simplifications had to be made to the circular net cages when modelling in the built-in DesignModeler geometry. The diamond shaped mesh was replaced by a square mesh to reduce the number of twines/elements.

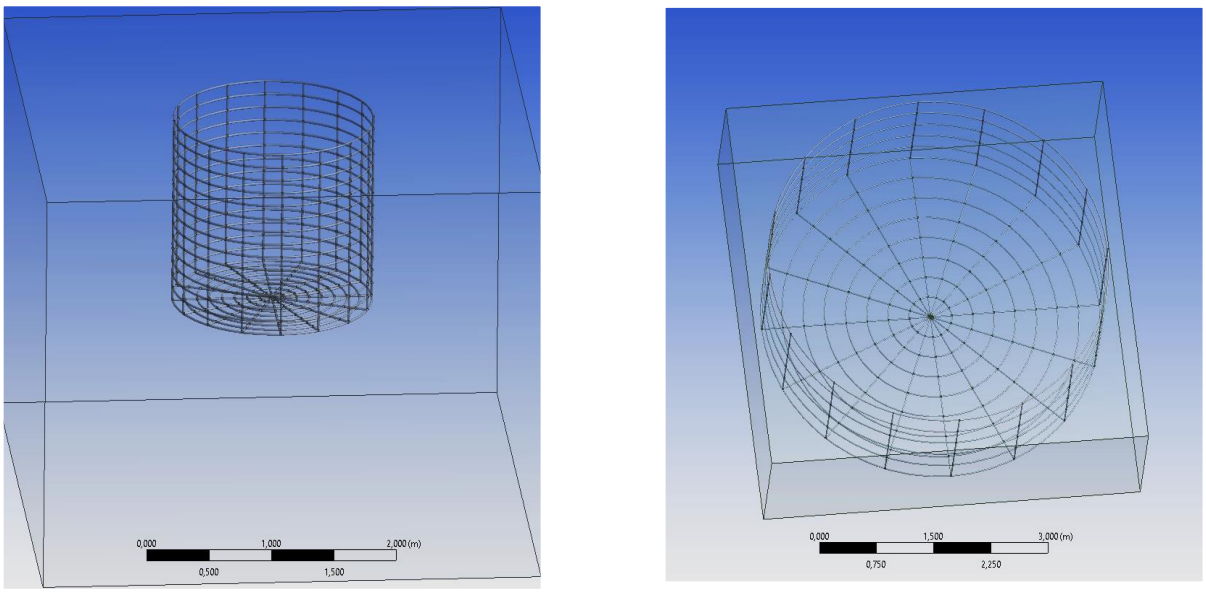

Figure 19 - Models of circular net cages made in DesignModeler. On the left: height 1,4m and diameter 1,6m. On the right: height 1,4m and diameter 4,8m. The square box surrounding the net cages is defined as the water domain.

The circular net cages were made of three-dimensional cylinders and tori with a diameter of 18 mm. The coordinates for the 16 points around the circular cages were found from vertexes I extracted from 3ds Max models I made for the two cages. The bottom was made by making a new plane placed at one of the end points of the circle and rotating cylinders around the circular cage.

The Fluent solution diverged while using a coarse mesh for these detailed geometries. The problem with these models is the number of elements generated from a finer mesh. Starting with the largest cage with a diameter of 4,8m, the number of elements/cells ranges from ~50 million with a freeboard and a draft, to over 70 million elements for a fully submerged cage. The high number of elements comes from the fluid-structure interface where the thin twines separates the water elements around the interface, as you can see on the illustration in figure 20. Before being able to process the net cages in ANSYS Fluent, both a ANSYS Academic Research license and the Lenovo ThinkStation P910 had to be acquired, as a ANSYS Student

License has a numerical limit of 512000 nodes/cells. The P910 was brought in to give additional computational power.

Reducing the net geometry to a diameter of 1,6m did not help as the number of elements was 42 million for a completely submerged cage with a fine mesh. While solving in ANSYS Fluent, both the computer CPU and the memory of the P910 got maxed out (100% usage) with the circular net cages. Solving the issue would require even more computational power or by reducing the number of elements generated by meshing.

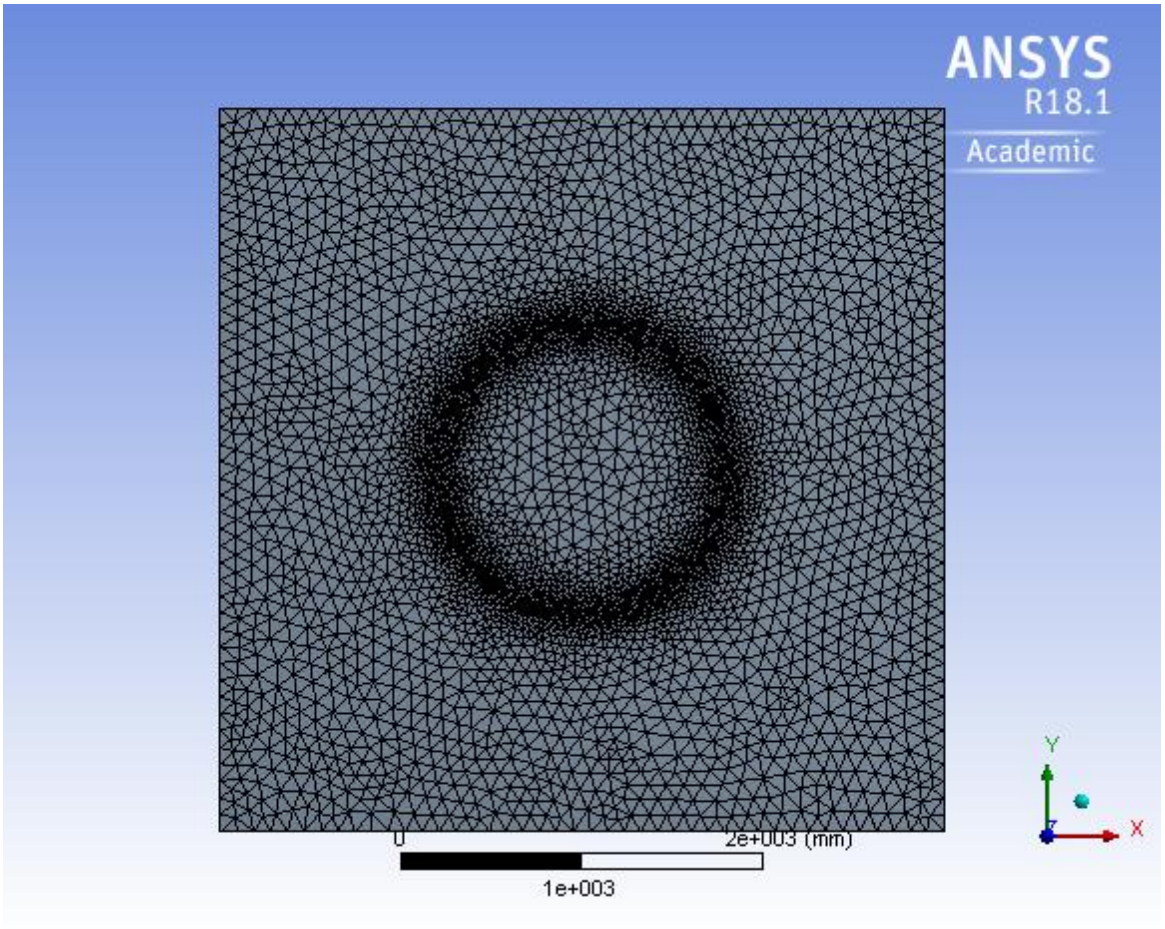

Figure 20 - Illustration of high number of element meshing for a circular cage.

Using a coarser mesh for the smaller net cage introduced an error that states “maximum cell skewness exceed 0.98” in the Fluent solver. According to ANSYS Help [33], high mesh skewness can lead to instability in the solver. The skewness problem was solved by increasing the number of elements by changing the mesh settings for both the relevance center and span angle center to medium, as well as improving the grid quality. The worst ~0.2% (19207 out of 9571081 cells) of the poor-quality cells were identified and processed over 1000 iterations to solve the issue. Still, the pressure could not be imported to static structural in neither the ANSYS custom system Fluid Flow (Fluent) -> Static Structural nor the modified FSI system, presented in figure 5. Changes to the mesh type from adaptive to proximity and curvature with coarse-medium-fine meshes could not solve the problem as the pressure still would not be imported or that the residuals would not converge. Hence, I made further simplifications to the netting, and built a net panel that refers to a section of the netting.

3.3 Finite element model of the net panel

The net panel is built as three-dimensional cylinders in DesignModeler geometry.
The net panel was created with the following properties:

Length of mesh side	54,4 mm
Twine thickness	3 mm+50% fouling = 4,5 mm
Beam thickness	4x Twine thickness = 18 mm
Twine cross-section area	254.47 mm^2

Table 3 - Geometric properties of the net panel.

Note that the length of mesh side is twice the maximum length presented in "Tabell 1" [34] p.20. As I combined 4 twines into each beam element, I increased the length so the mesh openings/solidity would not be too small.

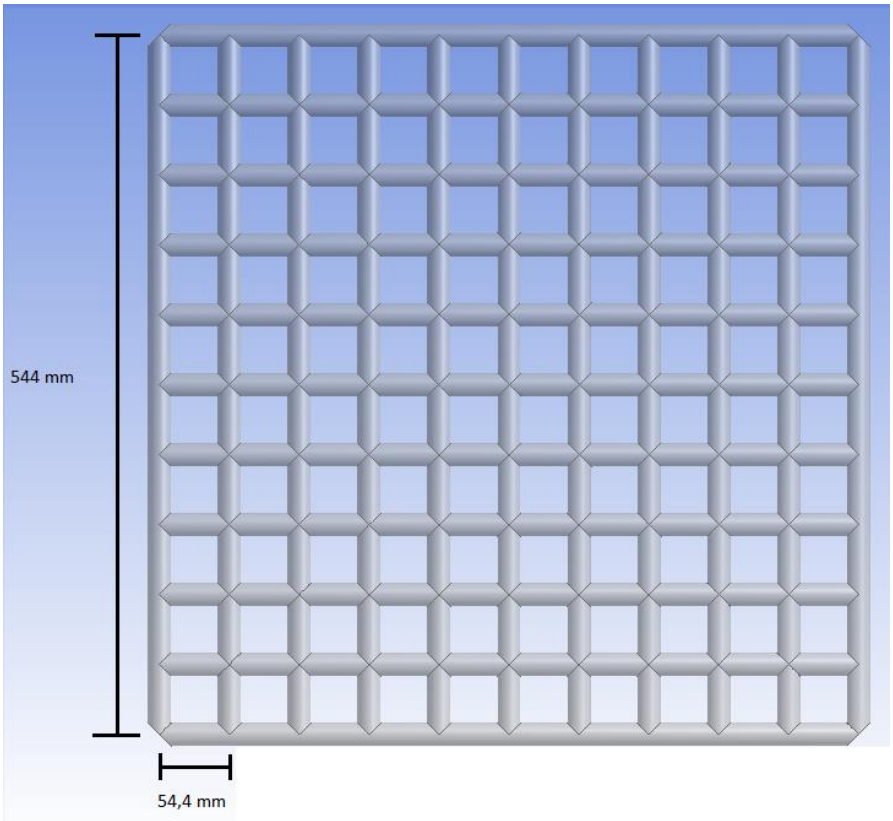

Figure 21 - Illustration of the net panel geometry. Bounding box length x=18mm, y and z=562mm.

The finite element model of the water mesh consists of 2767284 elements and 3858390 nodes. The mesh is generated with a CFD physics preference in the Fluent solver. Element sizing is decided by the size function proximity and curvature, with a medium relevance center, slow transition and a fine span angle center. The quality target skewness is by default 0.9, with medium smoothing. While meshing the water domain, the net panel is suppressed. Still, we can see an increased number of elements due to the fluid-structure interface which consists of 194 faces with a surface area of 0.54698 m^2 and a volume of 0.0026527 m^3. If the structure is not subtracted from the water domain, the water domain would just be a square mesh. The square mesh would have a small number of elements compared to the water domain with the fluid-structure interface. Another point to add to this is that, if the structure is not subtracted from the water, the water flow would not flow through the net.

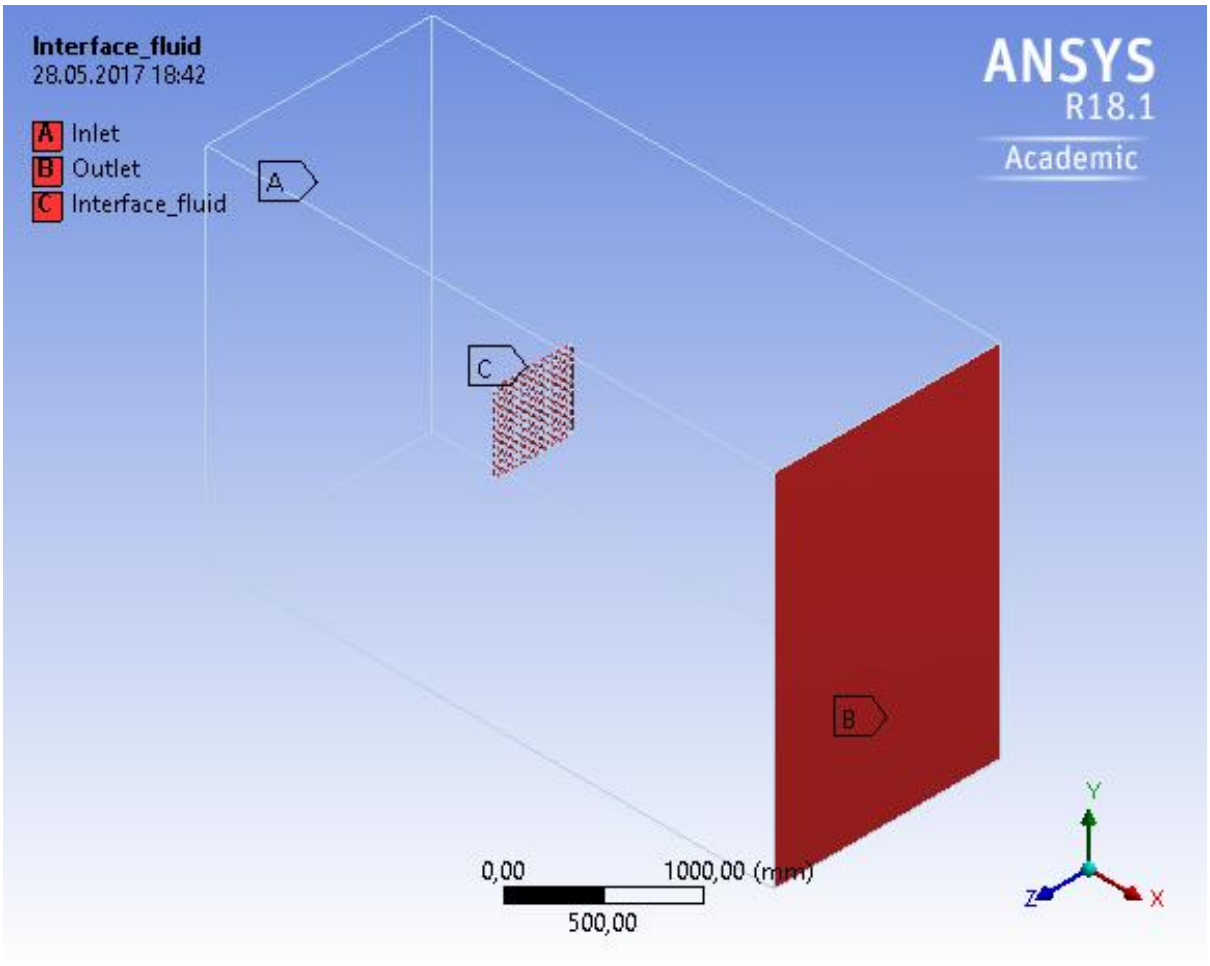

Figure 22 - Named selections of the geometry. The remaining walls around the water domain is defined as free surfaces.

The inlet is defined so that the flow travels in the direction of the positive x-axis, the y-axis is horizontal and the z-axis is vertical. The corners at each edge of the net panel are cut into one face to reduce the number of elements generated by meshing, as the circular end-points of the cylinders would further divide the water elements around the interface. Then, the Boolean unite operation is used to assemble all cylinders into one body; the net panel. The water domain is made in a rectangular shape with dimensions 4000x2544x1594 mm to make it symmetric around each side of the net, except in the x-direction where there is more space after the netting section to see the behavior of the flow lines. If the walls of the water domain are too close to the net panel, the flow lines will swirl more after deflection, which will affect the results. Finally, the Boolean subtract operation is used to subtract the net panel from the water domain, so ANSYS Fluent knows there is a solid body inside the water in Fluent meshing. If the net is not subtracted from the water domain, there is no CFD surface to import the pressure from Fluent to structural.

3.4 Processing the net panel in ANSYS Fluent

3.4.1 Fluent setup

The governing equations are discretized using the finite volume method (cell-centered) and solved using the CFD software ANSYS Fluent. A steady time simulation is used with a 3D pressure-based solver to enable the pressure-based Navier-Stokes solution algorithm. “The

pressure-based solver uses a solution algorithm where the governing equations are solved sequentially (i.e., segregated from one another). Because the governing equations are non-linear and coupled, the solution loop must be carried out iteratively in order to obtain a converged numerical solution." [35] Double-precision is specified in the Fluent launcher, this means that the residuals can drop as many as 12 orders of magnitude instead of the 6 orders of magnitude with single-precision before the residuals are converging. Parallel processing is enabled to make use of all 16 processors of the P910 and to reduce the computing time.

The turbulence/viscous model used is the realizable k-epsilon model with standard wall functions and default model constants; $C_{1\varepsilon} = 1.44, C_2 = 1.9, \sigma_k = 1.0$ and $\sigma_\varepsilon = 1.2$. The realizable k-epsilon model "is likely to provide superior performance for flow involving strong pressure gradients. For flow through and around a plane net, strong pressure gradients exist because of the blockage effect of the fishing net." [26] p.26.

Water-liquid is found from the Fluent material database, with a default constant viscosity of $0.001003\ kg/(m \cdot s)$ and a density of $1025\ kg/m^3$, for the cell zone conditions of the water domain. For the boundary conditions, the pressure is specified as constant, while the water velocity from the inlet is set to $0.1, 0.5, 1.0, 2.0$ and $5.0\ m/s$ to compare the behavior of the net panel of various materials at different flow rates. The inlet velocity is specified with default values, where the turbulent intensity set to 5% (medium intensity) and the turbulent viscosity ratio given by μ_t/μ is set to 10. The pressure outlet is specified with the same values for the backflow turbulent intensity and the backflow turbulent viscosity ratio.

The model has two mesh interfaces, one for the water cell zone and one for the solid net panel. Even though the interfaces have the same position and shape, the interface selected on the solid net panel will correspond to the solid cell zone, while the interface selected after suppressing the solid body in Fluent will only correspond to the fluid cell zone. The Fluent console states that the interface zones overlap for the mesh interfaces, and that this could adversely affect the solution. The two interface zones must be merged together into a single mesh before running the Fluent calculation. To merge the zones together, the coupled wall option is enabled in Mesh Interfaces under fluent setup. The coupled wall boundary at the interface is acting as a wall zone so the fluid cannot pass across the fluid-structure interface.

Before going on with the solution, the reference values are computed from the inlet and the seawater temperature is set to 275.95K (2.8°C, see assumptions) with the water domain as the reference zone.

3.4.2 Fluent solution settings

The pressure-velocity coupling method chosen is the default SIMPLE algorithm. "The SIMPLE algorithm uses a relationship between velocity and pressure corrections to enforce mass conservation and to obtain the pressure field." [36] The spatial discretization scheme for the gradient method is the default least squares cell based, while the pressure is defined with the default second-order scheme. The momentum, turbulent kinetic energy and turbulent

dissipation rate are carried out using a second order upwind scheme to improve the accuracy, as suggested by ANSYS Fluent when checking the case.

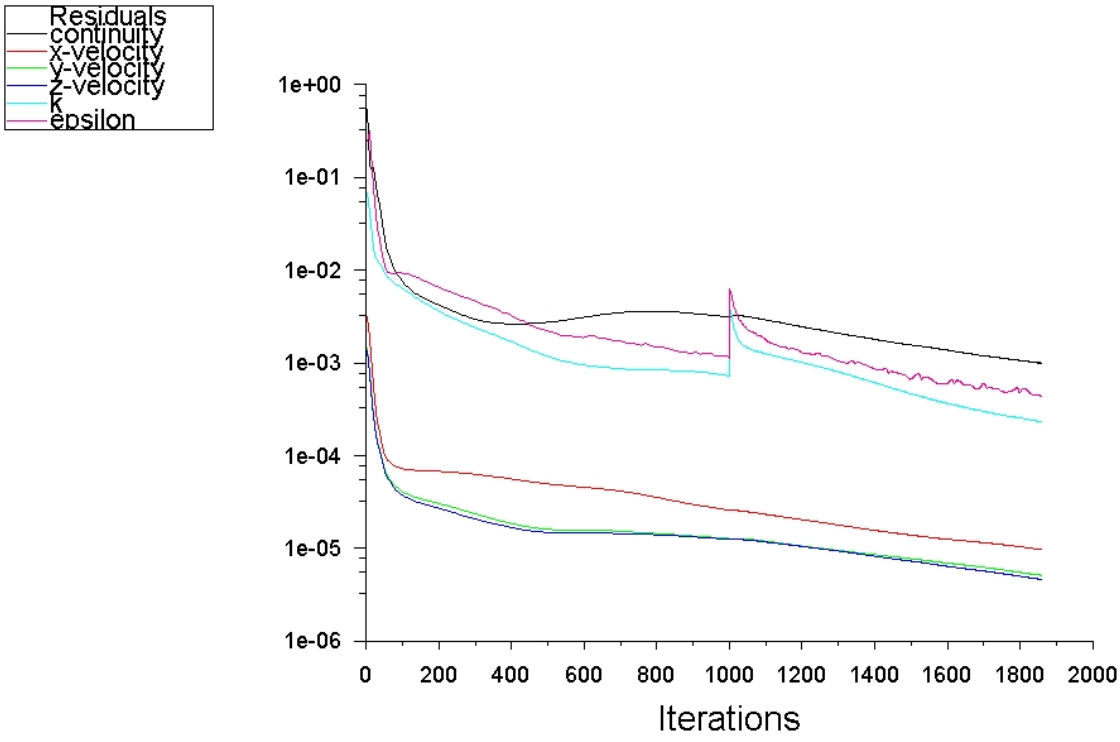

Figure 23 - Residual monitors converging with a water velocity of 0,1 m/s.

Note that the turbulent kinetic energy (k) and the turbulent dissipation rate (ε) are initialized with a first order upwind scheme. I did not use the second order upwind scheme for the cases where a good convergence was found by using a first order upwind scheme. Take the plot above as an example; I did not see the residuals converging with an inlet velocity of 0.1 m/s after 1000 iterations with first order, so I changed the spatial discretization scheme for the turbulent kinetic energy and the turbulent dissipation rate to second order for another 1000 iterations. Then, the solution met the convergence criteria at iteration step 1857. The solution is specified as having reached a converged solution when all residuals changes their value by less or equal to 0.001. The residuals did not meet the specified absolute criteria of 0.001 for the other velocities analyzed in this project, but they ran for 1000-2000 iterations until a converging behavior was found.

The first calculations were done with default under-relaxation factors for the solution controls, but the continuity equation did not converge. “For most flows, the default under-relaxation factors do not usually require modification. If unstable or divergent behavior is observed, however, you need to reduce the under-relaxation factors for pressure, momentum, k, and epsilon from their default values to about 0.2, 0.5, 0.5, and 0.5.” [37].
As these values for the under-relaxation factors still gave a divergent behavior, the under-relaxation factors were all reduced to 0,1. This solved the issue, and the solution converged. The solution limits and the advanced solution controls are set as default, where the V-cycle is used for the pressure equation in the pressure-based segregated algorithm and the flexible cycle is used for the momentum, turbulent kinetic energy and turbulent dissipation rate equations. A standard initialization method is used, computed from the inlet. The x-velocity is

the same as for the boundary conditions ($0.1, 0.5, 1.0, 2.0$ and $5.0\ m/s$), while the initial y- and z-velocity are set to 0 m/s, as the angle of attack for the flow is set perpendicular to the net panel.

3.5 Processing the net panel in static structural

Static structural analysis is used in ANSYS Workbench® to model the structural mechanics. The material properties are defined for each of the materials in Engineering Data, with Young's Modulus, Poisson's ratio and density (which must be specified when inertia forces are involved). The material properties used in this project are retrieved from RTP Company. Note that RTP Company list that: "This information is intended to be used only as a guideline for designers and processors of modified thermoplastics" for the properties of all materials used in this project.

Base polymer	**Description**	**Specific gravity [-]**	**Density [kg/m^3]**	**Tensile Modulus [MPa]**	**Global acc. (a_g) [m/s^2]**	**Mass of net panel [kg]**
Nylon PA6	Unreinforced base resin	1,13	1158,25	2758	1,2753	3,0725
Nylon PA6	30% glass fiber reinforced, heat stabilized	--	1350	9800	3,1105	3,5811
Polyethylene Terephthalate (PET)	30% glass fiber reinforced	1,56	1599	11032	5,4936	4,2416
Ester-based thermoplastic Polyurethane elastomer	30% glass fiber reinforced	1,44	1476	3103	4,3164	3,9154

Table 4 - Material properties retrieved from RTP Company. Ref: unreinforced Nylon [37], glass fiber reinforced Nylon [38], PET [39], Polyurethane [40].

goodfellow.com [32], professionalplastics.com [31] and Casanova, C. and W. Dwikartika [20] p.36. set the Poisson's ratio for nylon PA6 and PET-wire to 0.39, so the Poisson's ratio is assumed to be 0.39 for all materials in this project. The density of the materials is found from the specific gravity of the materials, except from nylon PA6 30% glass fiber reinforced as the density was given from RTP Company, using the following relation:

$$\rho_{material} = SG_{material} \cdot \rho_w \tag{24}$$

Where $SG_{material}$ is the specific gravity of the materials, while ρ_w is the density of seawater.

"The behaviour of the net cage can be dominated by non-linear effects due to very large deformations and materials with non-linear properties." [38] Synopsis p.4.
The pressure could not be imported with a nonlinear mechanical physics preference as the following error occurred; "An error occurred while transferring the load. The add-in did not generate any data to import." So, I made the following simplifications to the materials properties; each material is defined as linear elastic with isotropic elasticity derived from the Young's Modulus and the Poisson's Ratio. Now, by using the default mechanical physics

preference, the pressure imported without making any changes to the upstream component (Fluent solution).

3.5.1 Mechanical Model

The water domain is suppressed in the structural solver, so only the net panel is processed in the mechanical mesh. Using a fine mesh increases the computational time for importing the pressure, so I used a coarser mesh to reduce the computational time. The results are only affected by the mesh settings in a small scale because the net panel geometry is not as complex as the net cages. Element sizing is decided by the adaptive size function, with medium relevance center, slow transition and a coarse span angle center. Target quality is by default 0.05, with medium smoothing. The mesh transforms the single body into 32079 nodes and 15399 elements.

3.5.2 Structural solution settings

The governing equations are discretized using the finite element method (FEM) with the mechanical APDL solver target. The environment temperature is specified as 2.8°C. For the water velocities from 1.0 m/s and above, large deflection must be toggled on, since the deformation of the net panel is large compared to the model bounding box. “The message is displayed any time the software detects nodal deformations exceeding 10% of the model diagonal.” [39]. The remaining analysis settings are left to default.

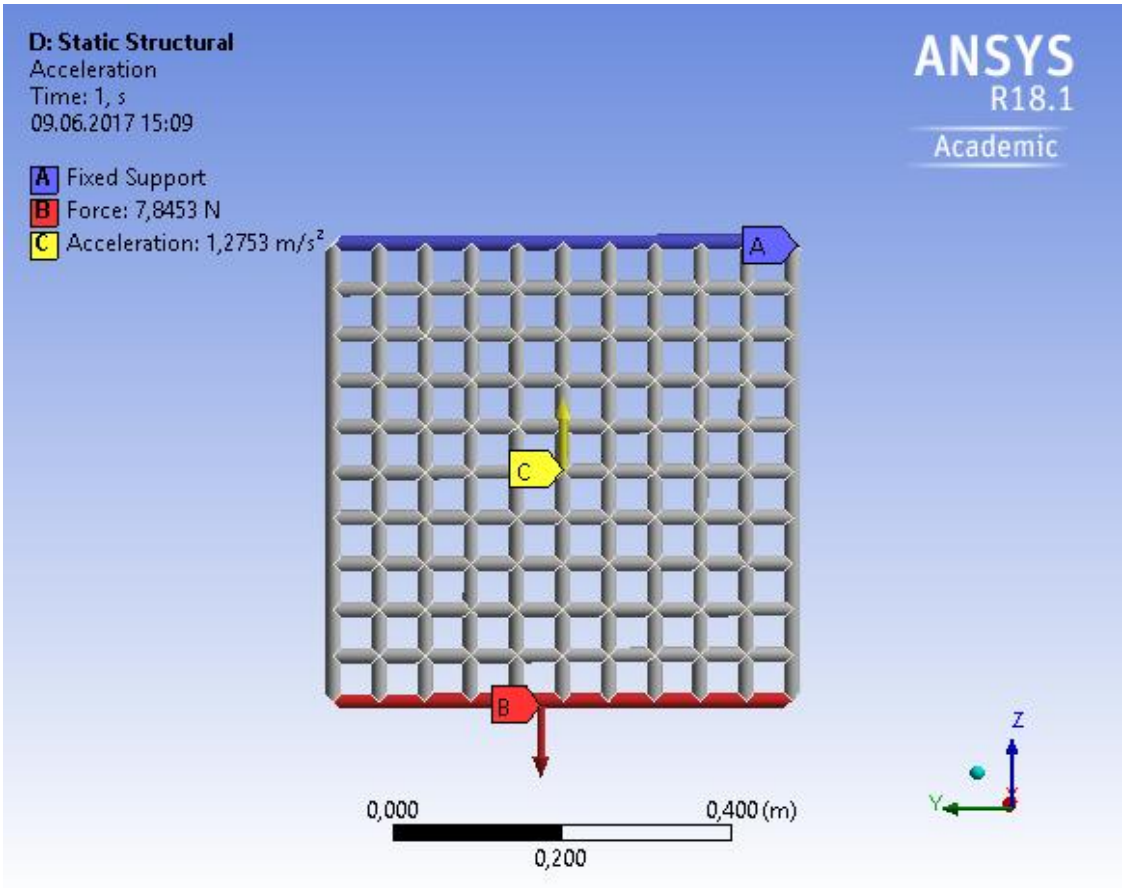

Figure 24 - The support and loading conditions specified for the net panel. Remember that the global acceleration changes with the netting material, here with unreinforced Nylon PA6.

The fixed support boundary condition is located at the top and at the two cut corners at the topside of the net panel, and keeps the selected faces from moving or deforming. The global acceleration boundary condition for the net panel is calculated by the buoyancy of the net and the gravity, presented in equation (7). The acceleration changes with the density of the materials used, and must be defined in the positive z-direction in the global coordinate system. The force represents a weight of 800 grams, with inspiration from H. Moe, et al. Model M1 [9] p.505, as used in the preliminary study.

The imported pressure is loaded to the net panel geometry by specifying the 194 faces of the net panel, and the fluid-structure interface is defined as the CFD surface.

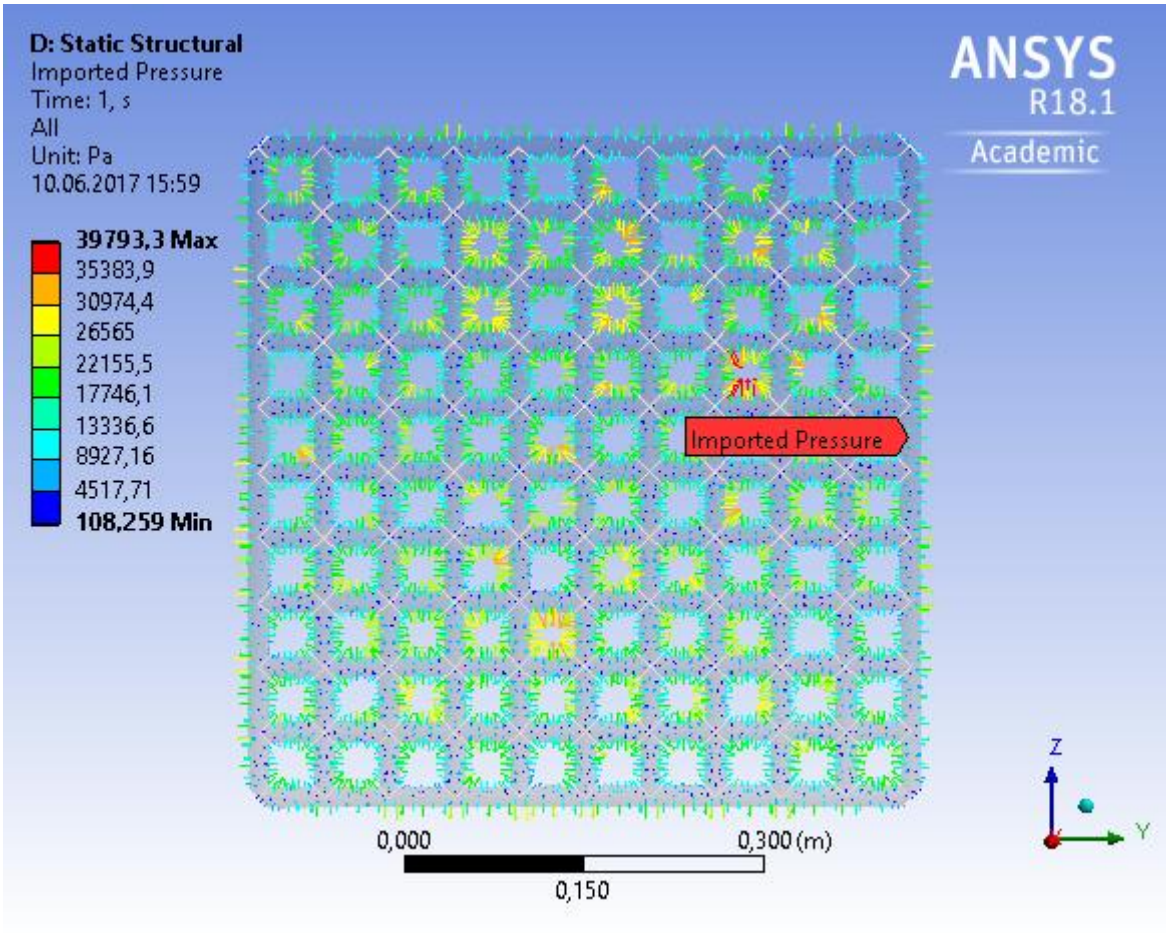

Figure 25 - Imported pressure with a water velocity of 5,0 m/s, seen from the outlet.

The imported pressure profiles for the remaining velocities can be found in the appendix.

4. Results & Discussions

4.1 Fluent results

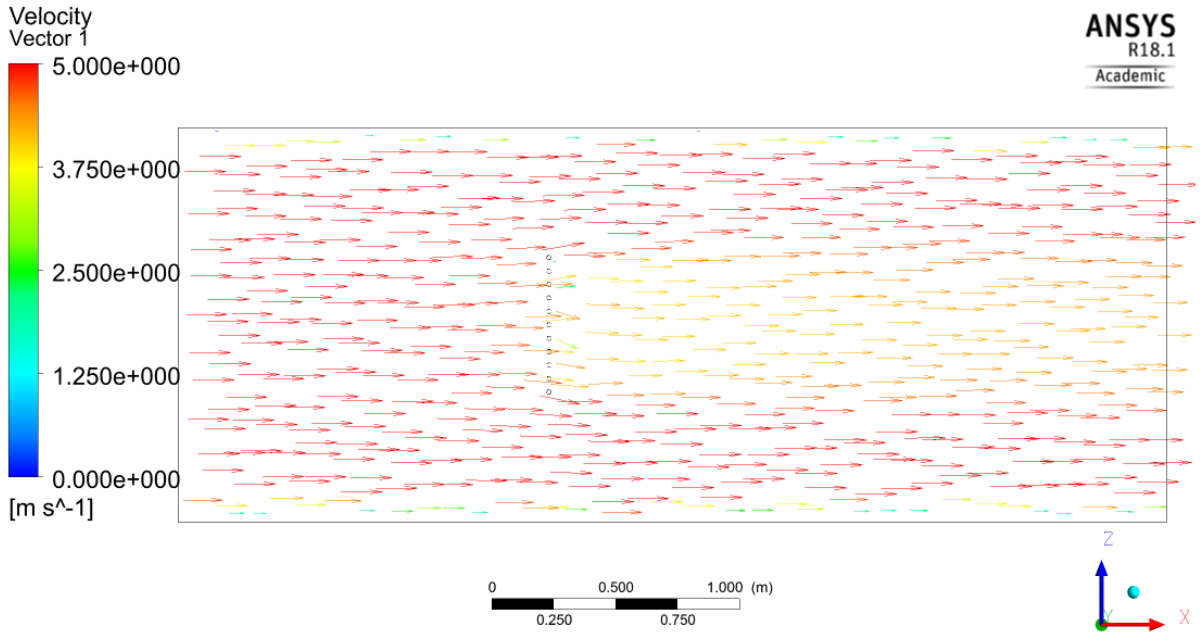

Figure 26 - Water velocity vectors with a water velocity of 5,0 m/s. 600 equally spaced points with a symbol size of 5.

To set up the water velocity vectors, a new plane is set in the results system (E) in the water domain. The plane is specified from the XZ plane in the centroid y = 272 mm of the water domain. The remaining velocity vector plots shows the same behavior for the other velocities, so they are not included in this report. The velocity streamline plots are also with 600 equally spaced points. The remaining streamline plots are found in the appendix.

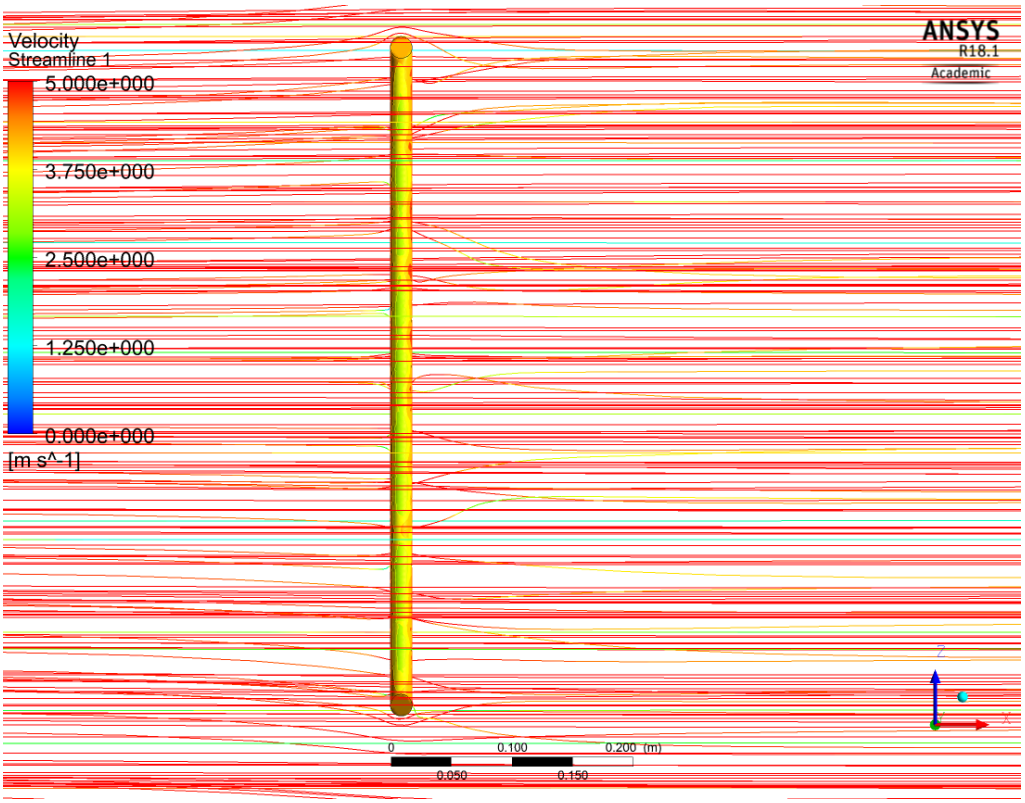

Figure 27 - Velocity streamlines deflected by the net panel with a water velocity of 5,0 m/s. The fluid-structure interface is shown with pressure contours.

4.2 Total deformation of the net panel

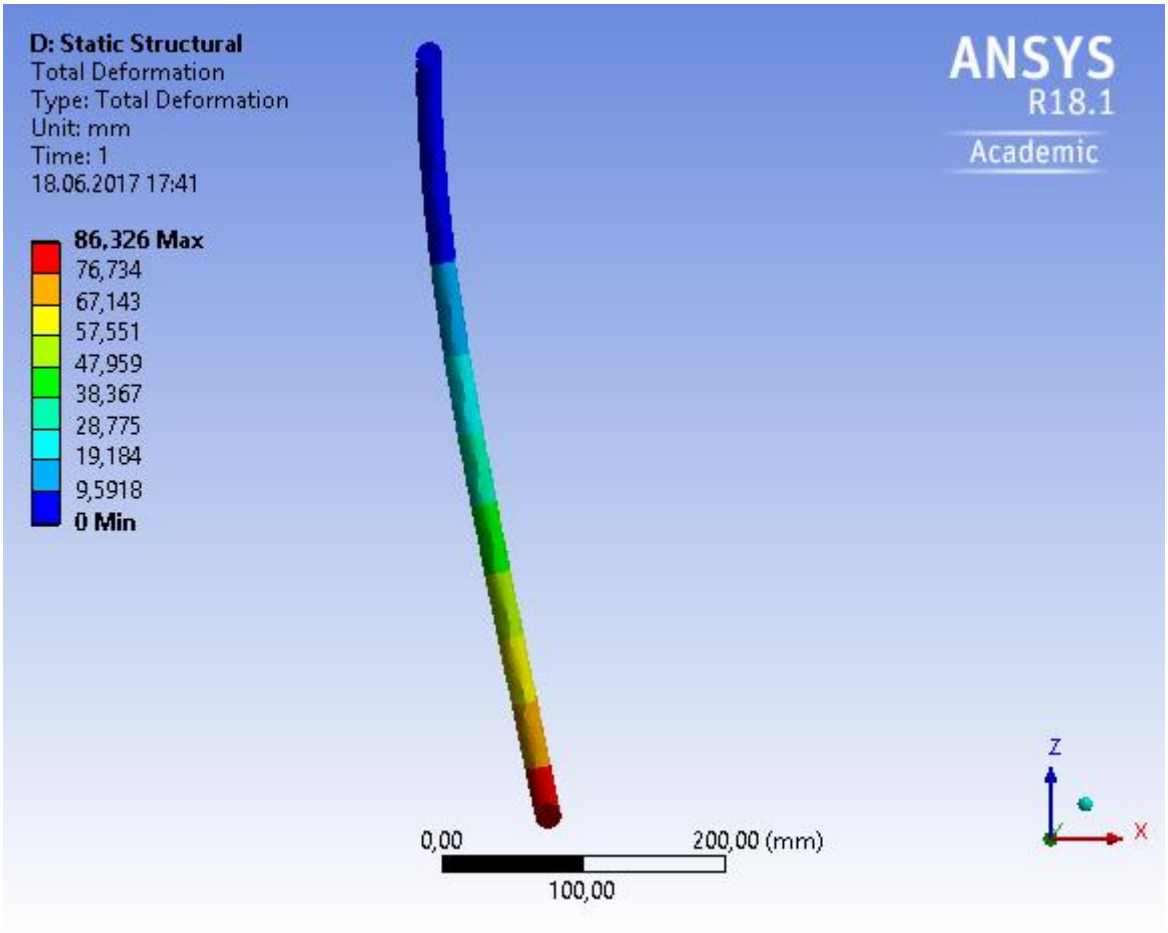

Figure 28 - Total deformation of the unreinforced Nylon PA6 net panel with a water velocity of 5,0 m/s (true scale).

The table below shows the maximum total deformation of the net panel with different materials, at each of the velocities:

Max. total deformation [mm]	Velocities				
	0,1 m/s	0,5 m/s	1,0 m/s	2,0 m/s	5,0 m/s
Nylon PA6 unreinforced	0,059388	1,0576	3,8757	15,053	86,326
Nylon PA6 reinforced	0,016781	0,29876	1,0912	4,2364	26,085
PET-wire	0,014903	0,26529	0,96898	3,7633	23,212
Polyurethane	0,052694	0,93837	3,441	13,38	77,452

Table 5 - Maximum total deformation of the net panel.

Note that: “A good water exchange will occur with a water velocity above 0.1 m/s. This is normally sufficient to supply enough oxygen and to remove fish excrement. However, the water currents should be below 1 m/s because velocities above this will result in very large forces on the cage structure and mooring system; in these situations, specially designed systems must be used.” [7] p.250.

4.3 Equivalent stress in the beam elements

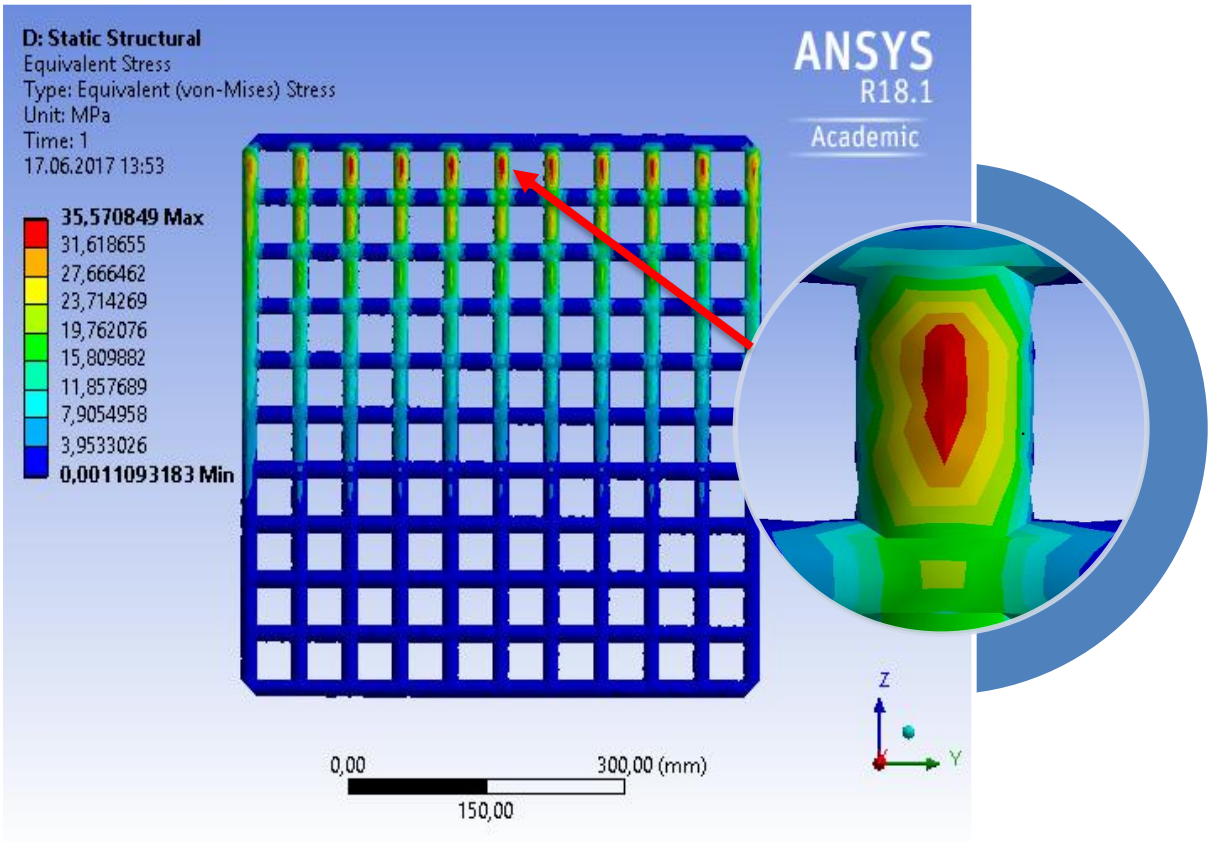

Figure 29 - Equivalent stress of the PET-wire net panel with a water velocity of 5,0 m/s, seen from the outlet.

The maximum equivalent (Von Mises) stress of the net panel with the different materials and velocities are listed in the table below:

Max. Equivalent stress [Pa]	Velocities				
	0,1 m/s	0,5 m/s	1,0 m/s	2,0 m/s	5,0 m/s
Nylon PA6 unreinforced	27318	408514	1477228	5739321	33924880
Nylon PA6 reinforced	29900	412146	1481051	5741841	35519847
PET-wire	34135	416246	1484826	5746084	35570849
Polyurethane	31810	412426	1480195	5743851	34114041

Table 6 - Maximum equivalent stress of the net panel.

Safety factors calculated from the max. equivalent stress at 5,0 m/s	Ultimate tensile strength [MPa]	Safety factor, $F_s = \frac{S_{limit}}{\sigma_e}$
Nylon PA6 unreinforced	76	2,24
Nylon PA6 reinforced	180	5,07
PET-wire	152	4,27
Polyurethane	72	2,11

Table 7 - Safety factor for the net panel with the different materials. Tensile strength limits retrieved from RTP Company. Ref: unreinforced Nylon [37], glass fiber reinforced Nylon [38], PET [39], Polyurethane [40].

4.4 Discussion

The water velocity would not be as linear as we have seen on the velocity streamlines in this study. In reality, components such as “tidewater current, wind-induced surface current, outbreak from the coastal current and spring flood because of snow and ice melting” [40] p.21. would contribute to the total current overview. The angle of attack of the water would most likely not be set perpendicular to the net panel. The fixed supports that holds the top faces in a fixed position during loading would also be able to move a bit in a real situation. These are all factors that could change how the deformation of the net looks like if we were to install it in a fish farm.

Judging by the results of this study, all the materials could be used for net cages. As mentioned in the introduction, fish welfare depends on a certain minimum volume within the net cage. For the more remote areas with higher velocities, the stronger materials like reinforced nylon PA6 and PET-wire would enable the net to better maintain its shape. According to the Norwegian Standards NS9415, the breaking strength of the net pens below surface must not fall below 65% of the initial strength of the net. In areas where there are less environmental loads in form of currents and waves, economic analyses should be performed to see what material is the most reasonable by considering the material costs and the total life span of the nets.

The materials must also be analyzed for toxicity. The toxicity affects both the fish welfare as well as the marine ecosystem. Finally, the problems I faced by importing the pressure could possibly be solved with an update to the ANSYS simulation program. There may be a bug in the system as I’ve used the same method for the circular cages and the net panels, while the import only worked for the net panels.

5. Conclusions

The following conclusions can be drawn from this study:

- Reinforced nylon PA6 and PET-wire have proven to be the strongest materials. In exposed areas with larger forces on the cage structure, you would benefit from choosing one of the two.

- I recommend further analyses of the SK one component polyurea from China Institute of Water Resources & Hydropower Research in Beijing for use in less exposed areas. The material has shown good qualities for aquaculture purposes compared with the untreated Nylon PA6, which is commonly used for net cages. However, cost to benefit analysis is required.

- Companies that supply net cage systems to the aquaculture industry do not openly share information about the material properties used in the net cages. So, the material properties used in this study may only be used as a guideline for how the different materials behaves when the fluid flow exerts the hydrodynamic forces on the net.

5.1 Future work

After the completion of my master's thesis, the following ideas could be initiated based on this study:

- Develop a method for a non-linear FSI analysis of net cages, using non-linear material properties. Possibly with the floating collar and bottom ring/sinker tube installed.

- Perform new analyses in co-operation with one of the suppliers of aquaculture technology with the material properties used in the industry and to test prototypes. Another possibility is to buy some material samples and analyze the material properties, as well as to perform a Xenon lamp aging test to see the elongation at break and time duration of the materials.

- Perform a mooring analysis with AquaSim (FEA) simulations to determine the environmental loads the mooring system are exposed to, in compliance with the Norwegian Standard NS9415.

References

1. SHARCNET:www.sharcnet.ca. *12.4.3 Realizable k-epsilon Model*. FLUENT 6.3 User's Guide 2006; Available from: https://www.sharcnet.ca/Software/Fluent6/html/ug/node480.htm.
2. Norge, S. *Fishing nets. Netting. Basic terms and definitions.* NS-EN ISO 1107 2003.
3. Norge, S., *Marine fish farms. Requirements for site survey, risk analyses, design, dimensioning, production, installation and operation.*, in *Planning and production of main components: General*. 2009, Standard Norge: standard.no. p. 33.
4. kikkonet.com. *Net Rolls & Panels*. 2016 [cited 2016 December 3]; Available from: http://www.kikkonet.com/net_rolls.php.
5. Norge, S., *Marine fish farms. Requirements for site survey, risk analyses, design, dimensioning, production, installation and operation.*, in *Use of environmental parameters*. 2009, Standard Norge: standard.no. p. 45.
6. www.seatemperature.org. *Tromsø average March sea temperature*. 2017; Available from: https://www.seatemperature.org/europe/norway/tromso-march.htm.
7. Lekang, O., *Aquaculture Engineering, Second Edition*. 2013: John Wiley & Sons, Ltd.
8. Moe-Føre, H., et al. *Structural response of high solidity net cage models in uniform flow*. Journal of Fluids and Structures, 65 2016; 180-195]. Available from: http://www.sciencedirect.com/science/article/pii/S0889974616303279.
9. Moe, H., A. Fredheim, and O.S. Hopperstad. *Structural analysis of aquaculture net cages in current*. Journal of Fluids and Structures, 26(3) 2010; 503-516]. Available from: http://www.sciencedirect.com/science/article/pii/S0889974610000289.
10. Maccaferri. *Aquaculture Nets/Cages*. 2016; Available from: http://www.maccaferri.com/applications/aquaculture-netscages/.
11. AkvaGroup. *Cage Farming Aquaculture*. 2016; Available from: http://www.akvagroup.com/Downloads/Cage%20farming%20%20EN.pdf.
12. I.J. Aarhus, e.a., *Kartlegging av ulike teknologiske løsninger for å møte de miljømessige utfordringene i havbruksnæringen*. 2011, SINTEF.
13. AkvaGroup. *Cage Farming Aquaculture*. 2015; Available from: http://www.akvagroup.com/downloads/cat_%20cage%20-%20engelsk%203_7.pdf.
14. T. Thorvaldsen, e.a., *The escape of fish from Norwegian fish farms: Causes, risks and the influence of organisational aspects*, in *Marine Policy*. 2015, Elsevier.
15. Zhiheng, S. *The SK one component polyurea and its application in hydraulic and hydropower project structures*. Available from: China Institute of Water Resources & Hydropower Research Beijing IWHR-KHL Co., Ltd.
16. Company, R. *RTP 1205 S-65D - Ester-based Thermoplastic Polyurethane Elastomer (TPUR/TPU) - Glass Fiber*. 2007; Available from: http://web.rtpcompany.com/info/data/1200S/RTP1205S-65D.htm.
17. I. Tsukrov, e.a. *Finite element modeling of net panels using a consistent net element*. Ocean Engineering, 30(2) 2003 [cited 251-271; Available from: https://www.researchgate.net/publication/223240933_Finite_element_modeling_of_net_panel_using_a_consistent_net_element.
18. Perng, Y.-Y., *Modeling Fluid Structure Interactions*. 2011, ANSYS, Inc.
19. ANSYS, I. *ANSYS Mechanical User's Guide*. 2013; Available from: http://148.204.81.206/Ansys/150/ANSYS%20Mechanical%20Users%20Guide.pdf.

20. Casanova, C. and W. Dwikartika. *Modeling of Aquaculture PET Net with the Use of Finite Element Method*. 2013; Available from: https://brage.bibsys.no/xmlui/bitstream/handle/11250/238738/653349_FULLTEXT01.pdf?sequence=3&isAllowed=y.
21. Invent, S.B.A. *Strength of Materials: Axial Loading*. 2016 December 15; Available from: http://engineering-references.sbainvent.com/strength_of_materials/axial-loading.php#.WFMAR_nhDyQ.
22. Edge, E. *Shear Stress Equations and Applications*. 2016 December 15; Available from: http://www.engineersedge.com/material_science/shear-stress.htm.
23. Hall, N. *Navier-Stokes Equations - 3-dimensional-unsteady*. 2015; Available from: https://www.grc.nasa.gov/WWW/k-12/airplane/nseqs.html.
24. Anderson, J.D., *Computional fluid dynamics - The Basics with Applications*. 1995: McGraw-Hill, Inc. 547.
25. ANSYS, I. *4.3.3.2. Transport equations for the realizable k-ε equation*. Theory Guide 4.3.3. Realizable k-ε Model Release 18.1; Available from: https://ansyshelp.ansys.com.
26. Zhao, Y.-P., et al. *Numerical simulation of the flow around fishing plane nets using the porous media model*. Ocean Engineering 2013 [cited 62; 25-37]. Available from: http://www.sciencedirect.com/science/article/pii/S0029801813000243.
27. Potyagaylo, S. and S.G. Loizou. *Online Adaptive Geometry Predictor of Aquaculture Fish-Nets*. 2014; Available from: http://ieeexplore.ieee.org/stamp/stamp.jsp?arnumber=6961505.
28. myn3wname(YouTube). *3ds max: Mesh modeling tutorial*. 2009 [cited 2016 December 3]; Available from: https://www.youtube.com/watch?v=aS5Axs3-RjM.
29. Lee, H.-H. *Finite Element Simulations with ANSYS Workbench 16* Chapter 1: Introduction 2016; Available from: http://myweb.ncku.edu.tw/~hhlee/Myweb_at_NCKU/ANSYS16.html.
30. W. Dwikartika, C.C., in *Modeling of Aquaculture PET Net with the Use of Finite Element Method*. 2013.
31. professionalplastics.com. *Mechanical Properties of Plastic Materials*. 2017; Available from: http://www.professionalplastics.com/professionalplastics/MechanicalPropertiesofPlastics.pdf.
32. goodfellow.com. *Polyamide - Nylon 6 (PA 6) - Material Information*. 2017; Available from: http://www.goodfellow.com/E/Polyamide-Nylon-6.html.
33. ANSYS, I. *28.3.1.1. SIMPLE vs. SIMPLEC*. Fluent 28.3.1. Choosing the Pressure-Velocity Coupling Method Release 18.1; Available from: https://ansyshelp.ansys.com.
34. Harboe, T. and O.F. Skulstad. *Maskeåpning, rømningsfare og fiskevelferd*. 2014; Available from: https://www.imr.no/filarkiv/2014/03/maskeapning_romningsfare_og_fiskevelferd.pdf/nb-no.
35. SHARCNET:www.sharcnet.ca. *25.1.1 Pressure-Based Solver*. FLUENT 6.3 User's Guide 2006; Available from: https://www.sharcnet.ca/Software/Fluent6/html/ug/node987.htm.
36. SHARCNET:www.sharcnet.ca. *21.4.3. Pressure-Velocity Coupling*. Release 17.0 [cited 2017 June 4]; Available from: https://www.sharcnet.ca/Software/Ansys/17.0/en-us/help/flu_th/flu_th_sec_uns_solve_pv.html.

37. SHARCNET:www.sharcnet.ca. *25.9.2 Setting Under-Relaxation Factors*. FLUENT 6.3 User's Guide 2006; Available from: https://www.sharcnet.ca/Software/Fluent6/html/ug/node1022.htm.
38. Moe, H. *Strength analysis of net structures*. Doktoravhandlinger ved NTNU, 1503-8181; 2009:48 2009; Available from: http://hdl.handle.net/11250/236414.
39. ANSYS, I. *The Deformation is Large Compared to the Model Bounding Box*. Mechanical User's Guide - Troubleshooting v.18.1; Available from: https://ansyshelp.ansys.com.
40. Norge, S., *Marine fish farms. Requirements for site survey, risk analyses, design, dimensioning, production, installation and operation.*, in *Site surveys: General*. 2009, Standard Norge: standard.no. p. 21.

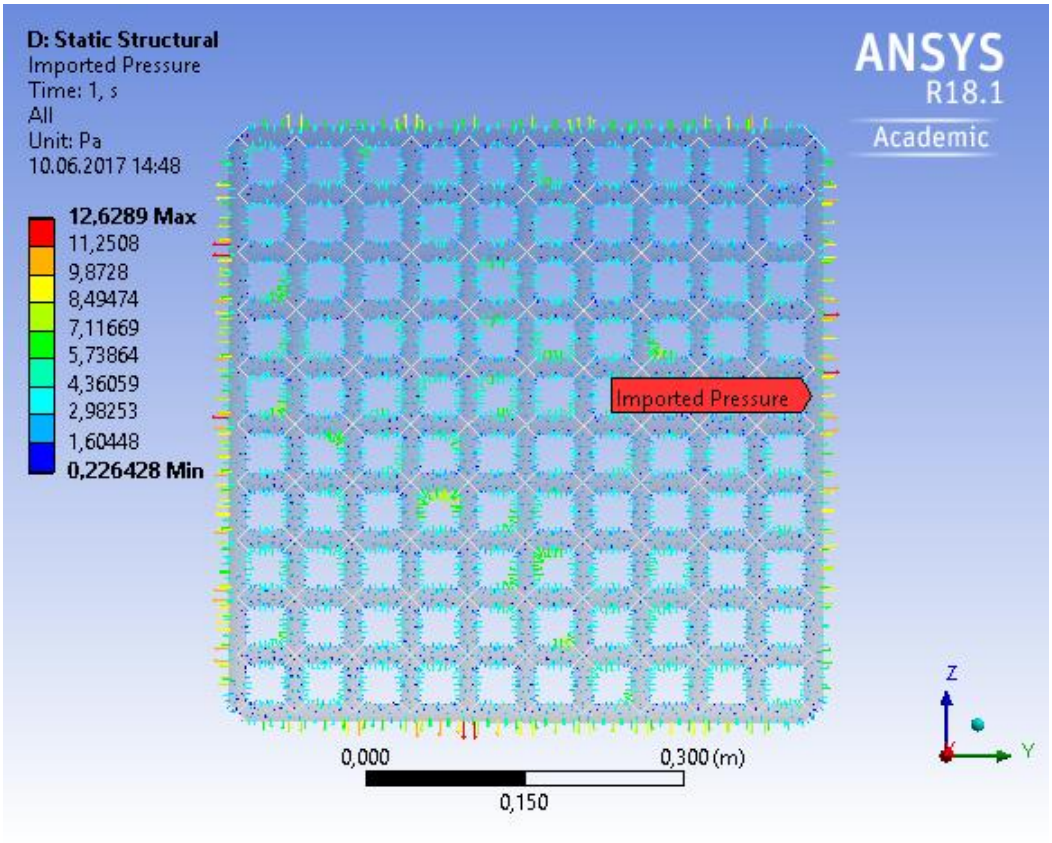

Figure 30 - Imported pressure with a water velocity of 0,1 m/s, seen from the outlet.

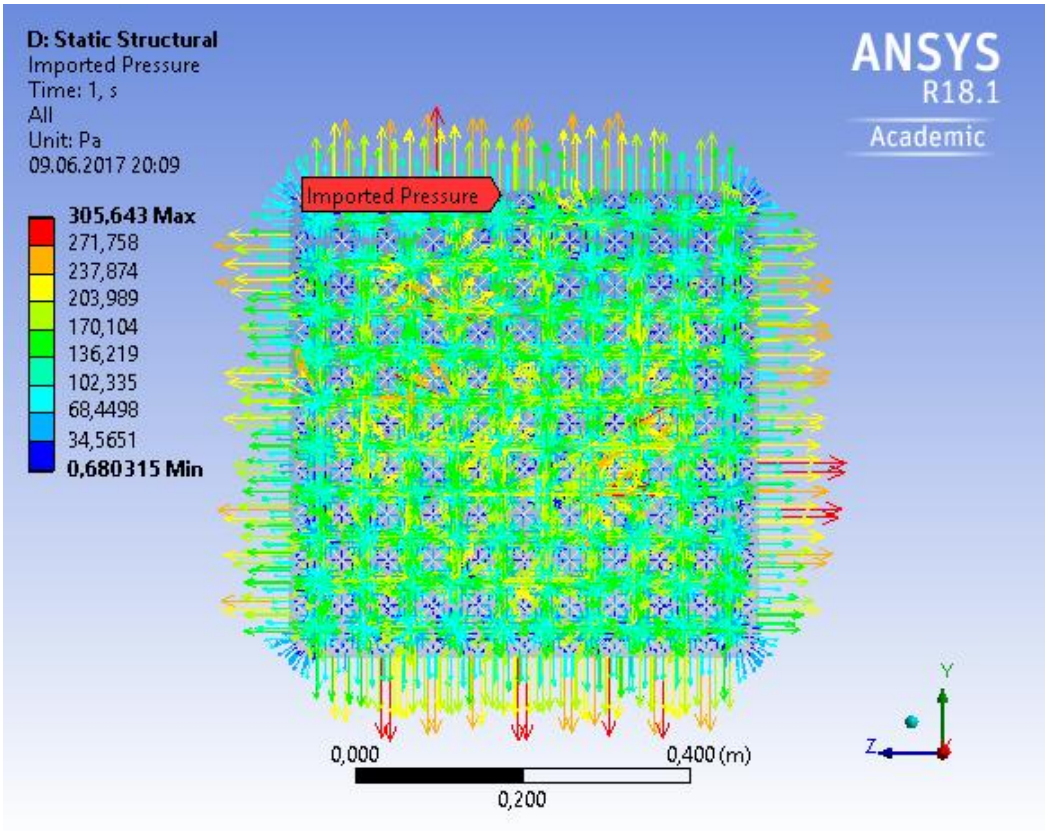

Figure 31 - Imported pressure with a water velocity of 0,5 m/s, seen from the outlet.

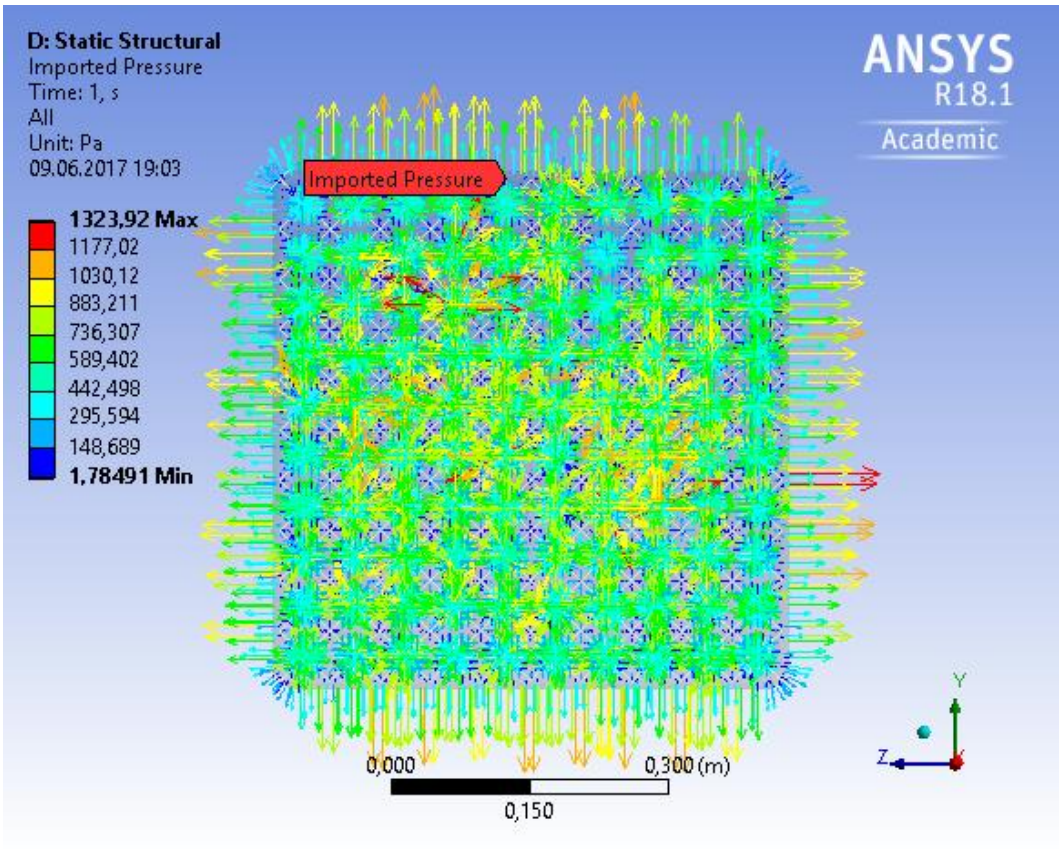

Figure 32 - Imported pressure with a water velocity of 1,0 m/s, seen from the outlet.

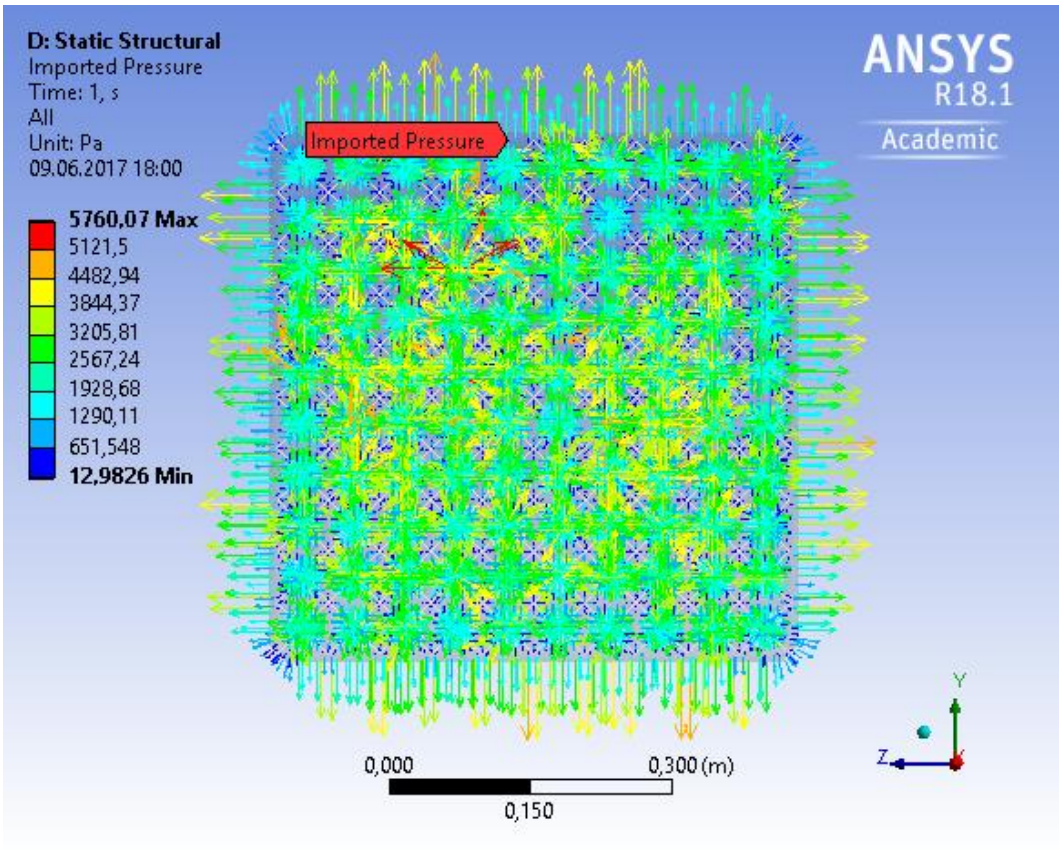

Figure 33 - Imported pressure with a water velocity of 2,0 m/s, seen from the outlet.

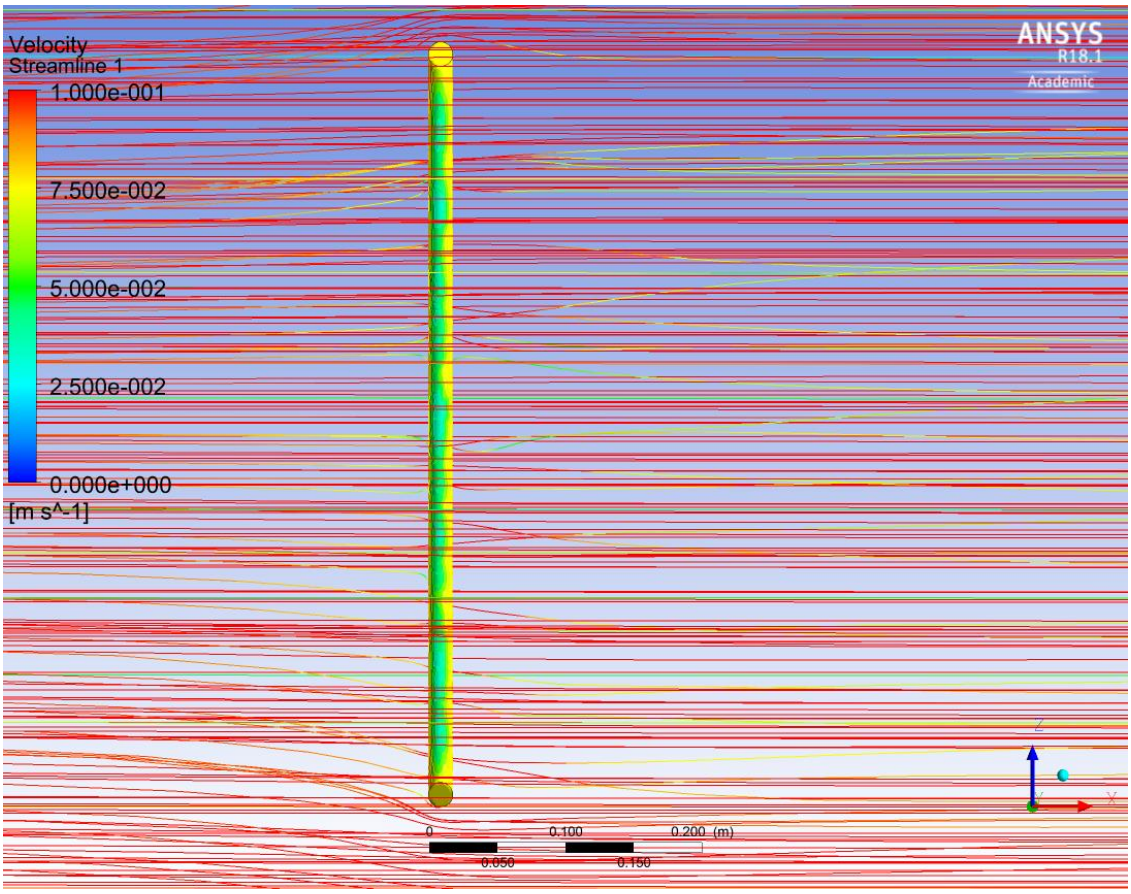

Figure 34 - Velocity streamlines with a velocity of 0,1 m/s.

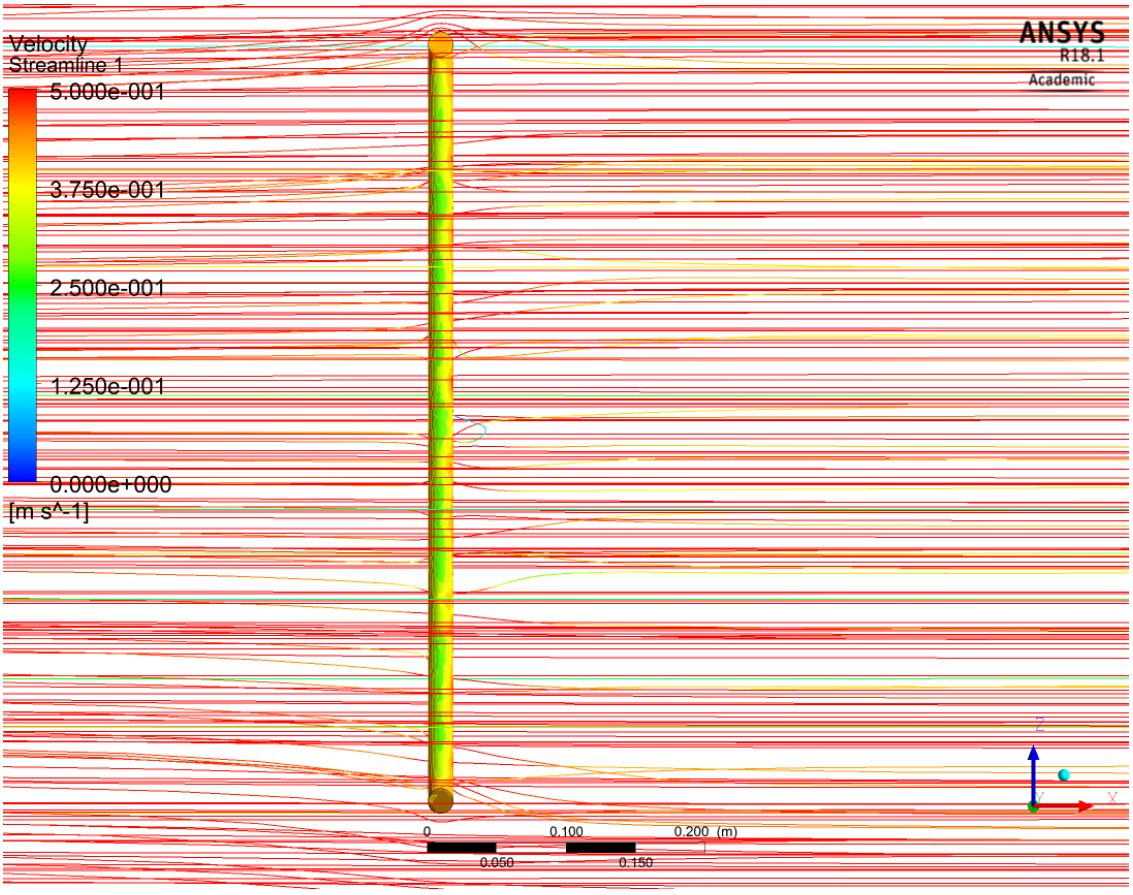

Figure 35 - Velocity streamlines with a velocity of 0,5 m/s.

Figure 36 - Velocity streamlines with a velocity of 1,0 m/s.

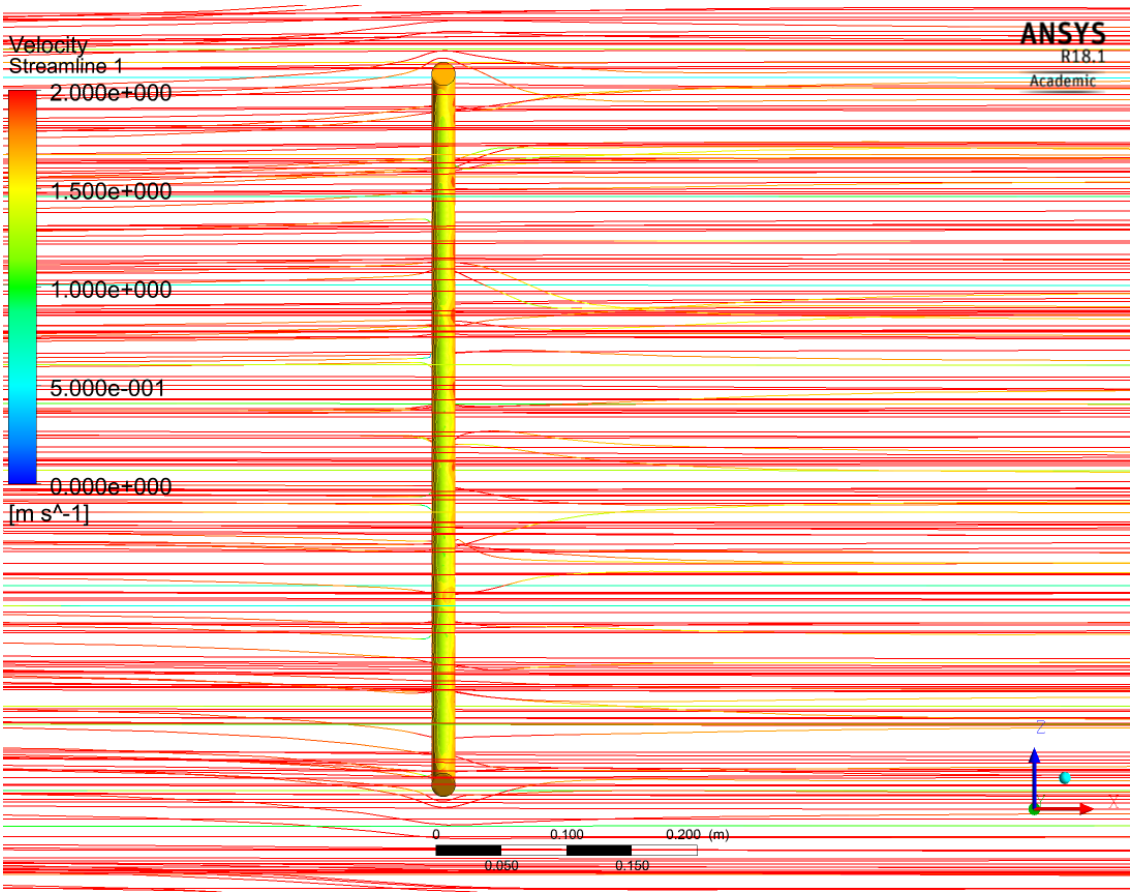

Figure 37 - Velocity streamlines with a velocity of 2,0 m/s.